Cell Reports
Physical Science

CellPress
OPEN ACCESS

Article

Can Industrial-Scale Solar Hydrogen Supplied from Commodity Technologies Be Cost Competitive by 2030?

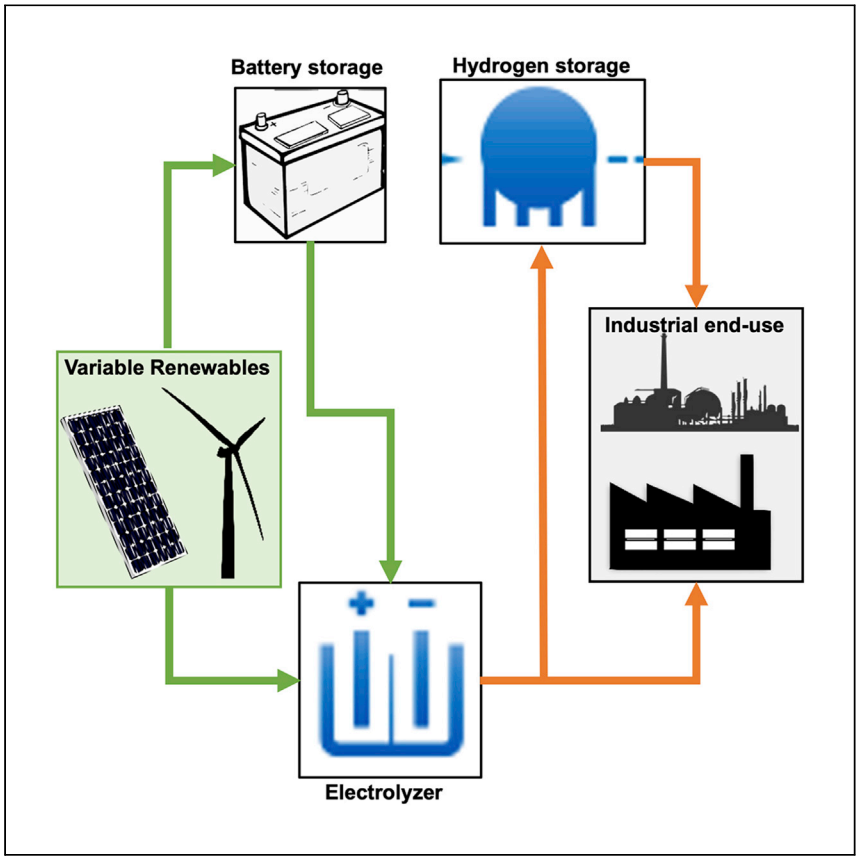

Identifying cost-effective, low-carbon H_2 production could accelerate the energy transition through decarbonization of end-use applications where direct electricity use remains challenged. Mallapragada et al. investigate the techno-economic outlook of industrial-scale H_2 supply produced from integrating commercially available PV, electrolyzer, and storage technologies across the continental United States.

Dharik Sanchan Mallapragada, Emre Gençer, Patrick Insinger, David William Keith, Francis Martin O'Sullivan

dharik@mit.edu

HIGHLIGHTS

Assesses cost of continuous H_2 supply via PV-electrolysis coupled with energy storage

Modeling least-cost design and operations shows value of oversizing PV capacity

Assesses cost of H_2 across continental United States for a range of component cost projections

Identifies combination of component costs and locations with levelized costs of $2.5/kg or less

Mallapragada et al., Cell Reports Physical Science *1*, 100174
September 23, 2020
https://doi.org/10.1016/j.xcrp.2020.100174

Cell Reports
Physical Science

CellPress
OPEN ACCESS

Article

Can Industrial-Scale Solar Hydrogen Supplied from Commodity Technologies Be Cost Competitive by 2030?

Dharik Sanchan Mallapragada,[1,5,*] Emre Gençer,[1] Patrick Insinger,[1] David William Keith,[2,3] and Francis Martin O'Sullivan[1,4]

SUMMARY

Expanding decarbonization efforts beyond the power sector are contingent on cost-effective production of energy carriers, like H_2, with near-zero life-cycle carbon emissions. Here, we assess the levelized cost of continuous H_2 supply (95% availability) at industrial-scale quantities (~100 tonnes/day) in 2030 from integrating commodity technologies for solar photovoltaics, electrolysis, and energy storage. Our approach relies on modeling the least-cost plant design and operation that optimize component sizes while adhering to hourly solar availability, production requirements, and component inter-temporal operating constraints. We apply the model to study H_2 production costs spanning the continental United States and, through extensive sensitivity analysis, explore system configurations that can achieve $2.5/kg levelized costs or less for a range of plausible 2030 technology projections at high-irradiance locations. Notably, we identify potential sites and system configurations where PV-electrolytic H_2 could substitute natural gas-derived H_2 at avoided CO_2 costs ($\leq$$120/ton), similar to the cost of deploying carbon capture and sequestration.

INTRODUCTION

Can solar-powered electrolytic hydrogen (H_2) supply industrial-scale quantities at sufficiently low cost by 2030 to allow large-scale, low-carbon production of energy-intensive products such as ammonia, carbon-neutral hydrocarbons, chemicals, or steel? This question is relevant for broader decarbonization efforts and in particular for industrial sectors, where progress regarding emissions reduction has been relatively modest (CO_2 emissions from the United States industrial sector decreased by 9% from 2008–2018 versus 26% for the power sector[1]), and direct use of low-carbon electricity may be difficult.[2–5] Although low-carbon H_2 production has historically attracted interest for decarbonizing transportation,[6] it might be more important in displacing fossil fuel use in industrial processes or as an intermediate in producing energy carriers such as ammonia or hydrocarbons. This observation is supported by recently announced pilot projects for use of electrolytic H_2 in steel production and petroleum refining.[7] Such large-scale demands for low-carbon H_2 will only be relevant under policies that drive rapid decarbonization with stringent carbon emission constraints. Assuming such policies, we examine the cost effectiveness of solar-powered electrolysis for industrial-scale (~100 tonnes/day) H_2 supply with high (95%) annual availability and its competitiveness with natural gas (NG) with carbon capture and sequestration (CCS).

Compared with distributed end uses, centralized end uses may provide a more appealing near-term opportunity for deploying emerging H_2 production routes,

[1]MIT Energy Initiative, Massachusetts Institute of Technology, Cambridge, MA 02139, USA

[2]Harvard John A. Paulson School of Engineering and Applied Sciences, Harvard University, Cambridge, MA 02138, USA

[3]Harvard Kennedy School, Harvard University, Cambridge, MA 02138, USA

[4]Orsted, Boston, MA 02110

[5]Lead Contact

*Correspondence: dharik@mit.edu

https://doi.org/10.1016/j.xcrp.2020.100174

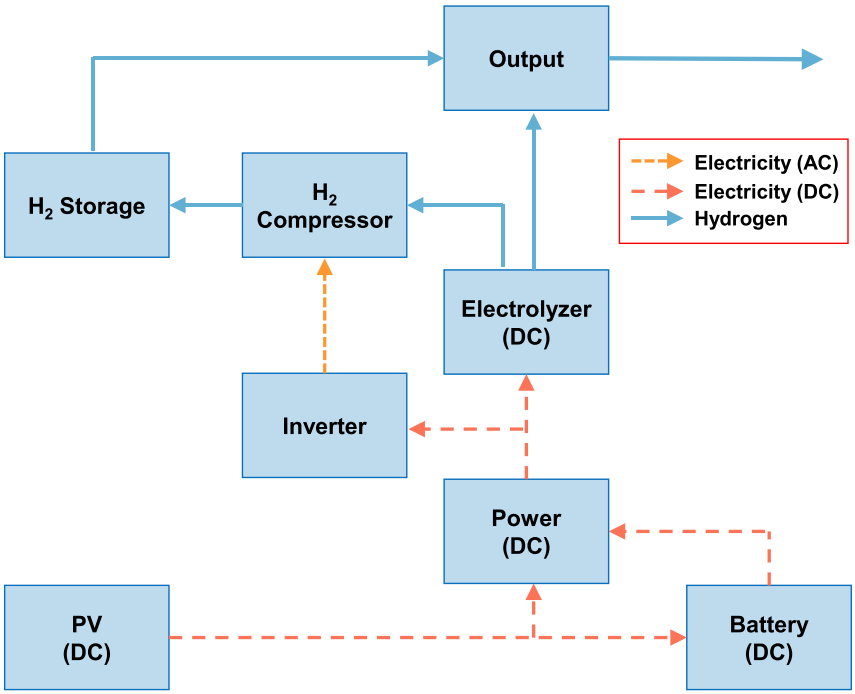

Figure 1. Schematic of the Integrated PV-Electrolysis-Storage Process for Continuous H_2 Production

Dotted lines indicate electricity flows, and solid lines indicate H_2 flows. AC, alternating current; DC, direct current.

like electrolysis, for a few reasons. First, existing H_2 demand is centralized, originating from petroleum refineries and chemical production facilities, whose typical H_2 consumption is supported by one or more production facilities producing H_2 on the order of 100 tons per day.[6] Second, centralized energy uses can potentially be served with on-site H_2 production that avoids the need for significant additional infrastructure for H_2 transport.[6] Third, targeting centralized end uses provides an opportunity to rapidly scale up commercially available but nascent technologies, like polymer electrolyte (PEM) electrolyzers, and, in the process, lower costs that could make them cost-effective for serving distributed end uses of H_2, like residential heating or transportation, in the future. Fourth, compared with direct electrification of distributed energy demands, like transportation, there is limited potential for direct electrification of many industrial operations, especially those relying on high-temperature heat inputs or direct use of fossil fuels as a feedstock (e.g., steel and ammonia), which makes H_2 use for these applications more appealing.

Here we focus on the techno-economic outlook in 2030 for round-the-clock electrolytic H_2 supply using dedicated solar photovoltaics (PV) installations and other commodity hardware (Figure 1)—battery energy storage, PEM electrolyzer systems, and gaseous H_2 energy storage—in pressure vessels or in geological formations, with the caveat that the latter may be geographically limited in its availability. We focus on 2030 for two reasons: industrial sector decarbonization will need to start by then to meet mid-century climate stabilization goals,[8] and it is far enough away that significant cost declines in electrolysis can possibly be realized but close enough that forecasts are meaningful. The rapid ongoing development of large-scale electrolysis[7,9–11] and the continued cost declines of utility-scale PV[12,13] make it more likely that solar H_2 systems developed by combining commodity hardware will be cheaper

than advanced first-of-kind integrated H_2 production systems within this time frame.[14] With respect to H_2 storage, currently available pressure vessel bulk H_2 storage is based on storing H_2 in pressurized tubes (~100 bar) that can be bundled together according to required storage volumes.[15,16] Unlike NG, storage of H_2 in pressure vessels requires specialized construction materials that are resistant to H_2 embrittlement and fatigue.[15] With growing interest in developing H_2 supply chains for refueling stations, pressure vessel bulk H_2 storage in pipe bundles is offered by several vendors (see Air Products and Chemicals Inc.[16] as an example) for commercial deployment. In contrast, large-scale H_2 storage in geological formations is practiced at scale, with five currently operating facilities across the world that use salt caverns and other hard rock formations to store thousands of tonnes of H_2 at pressures of around 100–200 bar.[17–19] Available literature regarding potential geological H_2 storage sites in the United States has focused on salt caverns, depleted oil and gas reservoirs, and aquifers distributed across the country, many of which are currently used for NG storage.[20]

For convenience, we model a strictly isolated PV-H_2 system (Figure 1) that does not account for possible interactions with the grid to sell excess PV electricity or import electricity during times of low PV output. Of course, any real-world system may choose to be grid connected, but our analysis provides a limiting case. In a world with policy sufficiently strong to justify industrial-scale low-carbon H_2 production, it may be reasonable to assume relative oversupply of electricity from variable renewable energy (VRE) at certain times of the day and strong economic incentives for low-carbon dispatchable electricity sources.[21] Policy supporting low-carbon fuel production would therefore also entail much larger growth of solar electricity generation, which is likely to intensify diurnal electricity price structures like the "Duck" curve currently observed in California,[22] where prices are depressed during hours of peak PV output and increase sharply at sundown. In this context, standalone systems, like that shown in Figure 1, may be advantageous because they can potentially mitigate the facility's exposure to intra-day and intra-year electricity price volatility. Additionally, the process shown in Figure 1 can also maximize the credits earned from low-carbon policies, such as the Low Carbon Fuel Standard (LCFS) in California, by relying exclusively on carbon-free electricity. The credit value for zero-carbon H_2 has been estimated at $2/kg.[23] Finally, we analyze PV rather than wind-based H_2 production because the former resource is more widely available and has a nearly an order of magnitude higher areal density and lower land use impact compared with wind generation (28 MW/km^2[2,24] versus 5 MW/km^2[25]).

Although techno-economic analysis of electrolytic H_2 production has been studied extensively in the literature, few studies have accounted for the temporal variability in the attributes of electricity supply (availability, emission intensity, and costs) and its effect on system metrics like levelized costs and emission intensity.[2,14,26–29] A key finding across these studies is that grid-based or grid-supported electrolytic H_2 production tends to be more cost effective than systems using VRE generation exclusively because they allow increased electrolyzer utilization and do not need additional investment in electricity generation equipment. For example, one study estimates the levelized cost for PV electricity-based electrolytic H_2 to be $6.1/kg when supplemented by grid electricity (priced at $0.07/kWh) and $12.1/kg when electricity is sourced entirely from PV.[14] However, electrolysis using on-site VRE generation and no storage versus using on-site VRE generation and grid-based electricity not only results in different H_2 production patterns over time but also potentially different greenhouse gas (GHG) emissions per kilogram of H_2 produced. Another study evaluated the cost of electrolytic H_2 across a variety of electricity

tariffs and with dynamic electrolyzer operation to be in the range of $2.6–$12.3/kg[30] but did not consider optimizing relative sizing of system components. Similarly, other studies that account for the effect of hourly operational variability on levelized costs of electrolytic H_2 did not optimize the relative sizing of system components (e.g., electrolyzer, PV, or wind capacity)[31–33] or consider the effect of onsite H_2 storage (G. Saur, 2011, Fuel Cell and Hydrogen Energy, conference).[35] Other analyses have focused on potential interactions of electrolyzers with the electric grid by flexibly scheduling power consumption and provision of energy and ancillary services.[29,36,37]

Our analysis of the cost-effectiveness of electrolytic H_2 production focuses on a facility (Figure 1), which relies exclusively on PV-sourced electricity to provide a continuous supply of H_2 for an industrial customer using on-site energy storage. A novel methodological contribution of this study involves the co-optimization of capacity of PV, electrolysis, energy storage, and other balance-of-plant components (e.g., inverter, H_2 compressor) to ensure continuous production while accounting for hourly variations in PV resource throughout the entire year and inter-temporal constraints governing equipment operation. This is accomplished by solving an integrated design and operations optimization model that models plant operations throughout the entire year at an hourly resolution (Experimental Procedures). Using this framework, we are also able to evaluate the trade-offs between energy storage as electricity or H_2 and the resulting effect on levelized cost under current and possible future technology cost and performance projections. Optimal sizing of system components is particularly important for VRE-dominant processes and systems where capital cost tends to dominate total costs.[29] For example, we find that the least-cost system design for the process shown in Figure 1 consistently sizes electrolyzer capacity smaller than the PV capacity across range of locations and cost scenarios. Additionally, we perform a spatial analysis of levelized H_2 production costs across the continental United States that, when considered with spatial distribution of existing H_2 demand, reveals regions with near-term deployment potential. For these candidate locations, we perform extensive sensitivity analysis to identify the impact of component cost and performance parameters and system factors, like plant annual availability, on achieving costs of $2.5/kg or less. The threshold value of $2.5/kg is near the higher end of the range of estimated levelized costs for H_2 production from NG with CCS ("blue H_2"), either via steam methane reforming (SMR) or autothermal reforming (ATR) approaches. There is a wide range of cost estimates for blue H_2 produced in central facilities in the literature, from $1.2/kg to nearly $3/kg, primarily because of varying assumptions about NG prices, cost of capital, and cost of CO_2 transportation and storage.[6,38–42] Incidentally, another assessment of the long-term cost competitiveness of H_2 to serve various end-use sectors also highlights $2.5/kg as a key cost benchmark.[42] Finally, we compare our results against the costs of NG-based H_2 production and conclude by noting the main implications and areas of future work.

RESULTS

Design and Cost Outcomes for a Plausible 2030 Cost Scenario

Figure 2 highlights the cost-optimal system design trends to produce H_2 round-the-clock at 4.17 tonnes/h (or 100 tonnes/day) across nearly 1,500 locations in the United States for the 2030 cost scenario defined in Table 1. These results are based on modeling a full year of plant operations at an hourly resolution, with PV resource characterized using typical meteorological year (TMY) data (Experimental Procedures; Note S2). Here we define "round-the-clock" to correspond to an annual plant

Please cite this article in press as: Mallapragada et al., Can Industrial-Scale Solar Hydrogen Supplied from Commodity Technologies Be Cost Competitive by 2030?, Cell Reports Physical Science (2020), https://doi.org/10.1016/j.xcrp.2020.100174

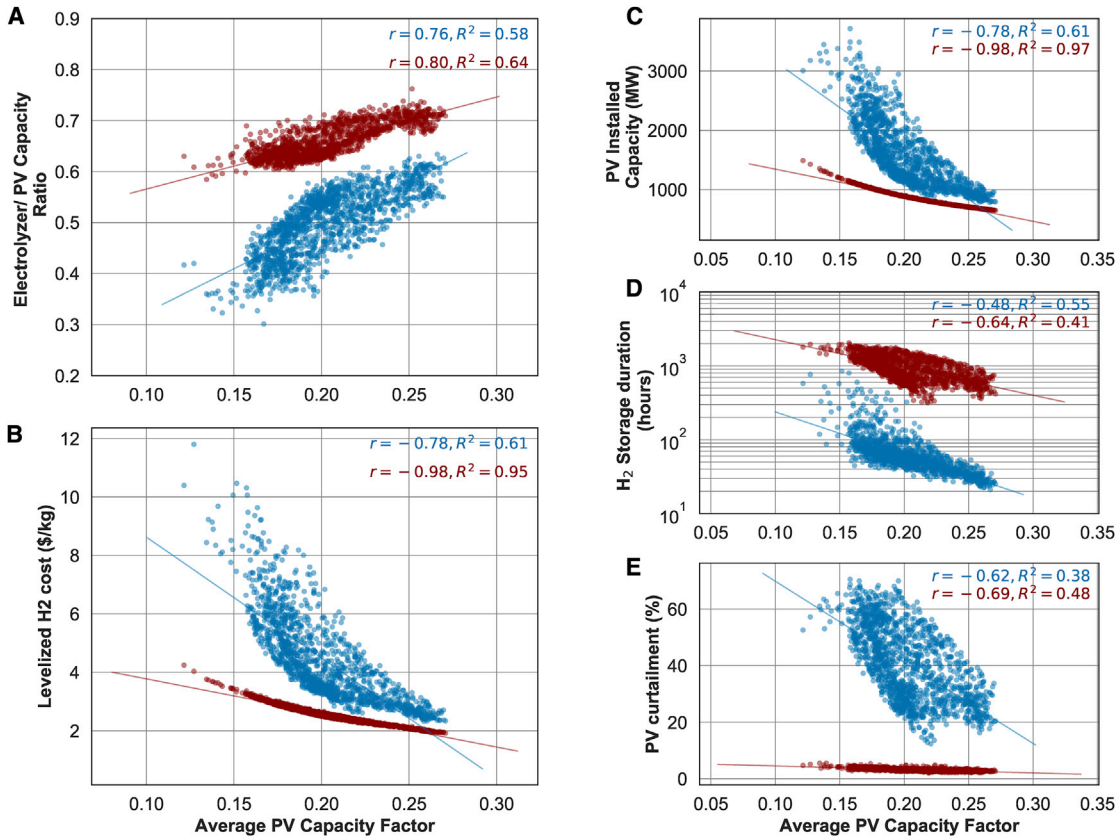

Figure 2. Least-Cost Design Trends for Continuous H_2 Supply from PV-Electrolysis + Storage across the Continental United States

Results correspond to nameplate H_2 production capacity of 100 tonnes/day (4.17 tonnes/h, 10% hourly tolerance) and 95% annual availability for various locations in the United States under the 2030 cost scenario with pressure vessel (blue) and geological H_2 storage (red) defined in Tables 1 and S4. Each point represents the design outcome for a different location in the United States, and the line corresponds to the least-squares linear fit of the data.

(A) Ratio of installed electrolyzer capacity to PV capacity.

(B) Levelized H_2 production cost ($/kg).

(C) PV installed capacity (megawatts).

(D) H_2 storage duration (h).

(E) PV curtailment as a percentage of available generation.

r, correlation coefficient; R^2, coefficient of determination of the linear fit shown for each figure. PV availability was characterized using TMY insolation data from the National Solar Radiation Database.[57] Duration of H_2 storage was calculated by dividing the capacity of installed H_2 storage (in tonnes) with the design flow rate (4.17 tonnegs/h).

availability of 95% (defined in Table 1) while allowing hourly H_2 supply rates to vary within 10%. The 2030 cost scenario was developed based on component cost projections in the literature and includes (1) PV capital cost of $500/kW (based on direct current [DC] capacity), which is plausible according to available projections;[12,43,44] (2) a 62% decline in capital costs for electrolyzer systems from their current levels of $800/kW (for multi-MW-scale systems[10,11,45]), which is the lower end of projections available in the literature[10,11,46,47] (see Note S2 for further details); (3) an increase in electrolyzer efficiency from current estimates of 58% to 70% on a lower heating value (LHV) basis[37]; (4) a 33% reduction in capital cost of pressure vessel H_2 storage compared with current (2020) cost estimates.[48] (the 2030 capital cost estimate is based on adjusting costs for pipe storage of NG [maximum pressure of 100 bar][15] to account for the different volumetric energy density of H_2 and NG); and (5) a lower range of capital costs reported for geological H_2 storage that is consistent with the large storage volumes being considered here[17–19] (see Table S5 for a brief

Table 1. Key Technology Performance and Cost Assumptions for 2020 and 2030 Scenarios and Sources

Parameters	2020	2030	References/Explanation
Capital Costs			
PV ($/kW DC)	850	500	single-axis tracking system with 0° tilt from horizontal; 2020 costs based on lower range of values noted in 2018 in the United States (see Figure 8 of Bolinger et al.[59]); 2030 estimate based on projections by Bloomberg New Energy Finance,[12] National Renewable Energy Laboratory[43], and Mallapragada et al.[44]
Electrolyzer, PEM ($/kW)	800	300	2020 costs based on cost estimates reported from multiple sources[9–11,45,46] and Figure 4 in Fuel Cells and Hydrogen Joint Undertaking[47]; 2030 costs based on lower end of projections for PEM systems[10,11,46,47]
Pressure vessel H_2 storage ($/kg)	516	345	pressurized pipes (100 bar); 2020 costs[48]; 2030 costs based on NG storage while accounting for H_2 volumetric energy density[15]
Geological H_2 storage ($/kg)	33	3	salt cavern (100 bar); 2020 costs from Ahluwalia et al.[48]; 2030 costs based on lower range of reported costs[19,60], consistent with large-scale storage volumes (see Table S5)
Compressor ($/kW)	1200	1200	Parks et al.[61]
Battery storage power ($/kW)	589	477	Low-end costs estimates for 2020 and 2030[13]
Battery storage energy ($/kWh)	206	77	Low-end costs estimates for 2020 and 2030[13]
FOM Costs (% of Capex)			
PV	1%	1%	National Renewable Energy Laboratory[43]
Electrolyzer	7%	5%	includes annualized stack replacement cost; 2020 values from Eichman et al.[37]; 2030 values based on International Renewable Energy Agency[28]
H_2 storage	1%	1%	Penev and Hunter[62]
Compressor	4%	4%	Penev and Hunter[62]
Operational Parameters			
Flow rate, minimum hourly utilization factor	4.17 tonnes/h, 90%		assumption
Annual plant availability	95%		Percentage of hours when facility is supplying H_2; similar to NG-based H_2 production facility
Electrolyzer efficiency, LHV (%)	58%	70%	2020 value based on International Energy Agency[6]; future values based on Table 2 in Eichman et al.[37] and range of values cited in Table 3 of International Energy Agency[6]
Battery storage round-trip efficiency (%)	92%		assumption
H_2 compression electricity input (kWh/kg)	1.0		energy input for 30 to 100 bar compression[15]

Remaining input parameters and their justification are provided in Table S4. Electrolyzer FOM costs reflect the estimated annualized cost of stack replacements based on a current cell stack life time of 5 years[6,47] and a project lifetime of 20 years (Note S2). DC, direct current; LHV, lower heating value. All dollar values are 2016 United States dollars unless noted otherwise.

literature summary of bulk H_2 storage capital costs). Although the sensitivity of system outcomes to alternative future component cost and performance assumptions are explored in more detail in the next section, here we present the major system design trends and favorable locations for initial deployment of PV-electrolytic H_2 based on the 2030 cost scenario described above and in Table 1.

Across locations and the two types of H_2 storage, the electrolyzer size is estimated to be less than the PV capacity because peak PV availability, such as with capacity factors greater than 90%, occurs for only less than 100 h of the year across locations (Figure S2). This finding, also observed in the case of the 2020 cost scenario (Figure S1), is in contrast to prior techno-economic assessments of electrolytic H_2 production,[6,14,27,28] which universally assume electrolyzer capacity to be equal to PV capacity irrespective of location or production requirements and, consequently, overlook the cost savings resulting from oversizing PV arrays. Smaller electrolyzer capacity relative to PV array leads to unutilized PV generation at hours of peak output (Figure 2E), but part of the "lost" H_2 production during the peak hours can be offset by increasing electrolyzer utilization during the "shoulder" hours; i.e., hours on either side of the hours with PV peak output. The cost

Please cite this article in press as: Mallapragada et al., Can Industrial-Scale Solar Hydrogen Supplied from Commodity Technologies Be Cost Competitive by 2030?, Cell Reports Physical Science (2020), https://doi.org/10.1016/j.xcrp.2020.100174

savings from oversizing the PV array relative to the electrolyzer is reinforced by the finding that the size of the electrolyzer relative to the PV array is positively correlated with the average PV capacity factor, as shown in Figure 2A. Regions with a higher PV capacity factor, synonymous with lower PV installed capacity (Figure 2C) and a greater number of hours of peak PV availability in a day, rely predominantly on these hours to produce the majority of daily H_2 requirements because the ability to produce H_2 during the shoulder hours is limited by PV power output (Figure S3). The opposite is true in the case of regions with a low PV capacity factor that are synonymous with larger installed PV capacity and, consequently, more PV generation during shoulder hours.

The cost of H_2 storage also affects electrolyzer sizing, with higher relative electrolyzer capacity (58%–76% of PV capacity) in the case of inexpensive geological H_2 storage compared with pressure vessel H_2 storage (30%–63% of PV capacity). The availability of low-cost H_2 storage (i.e., geological) makes it cost effective to use more of the PV electricity supply whenever it is available and store the produced H_2 for providing supply at other times. Consequently, system design with geological H_2 storage leads to larger relative electrolyzer size (Figure 2A), lower PV installed capacity (Figure 2C), greater H_2 storage capacity (Figure 2D), and lower PV curtailment (Figure 2E) compared with design outcomes with more expensive pressure vessel H_2 storage. PV curtailment predominantly occurs in the summer season (Figure 3), whereas plant operation in the winter nearly utilizes all available PV generation and even includes scheduled production downtimes, as illustrated in Figure 3, to minimize H_2 storage requirements and costs.

Despite the prevalence of PV curtailment (Figure 2E), battery storage is not chosen as part of the system design across any of the locations for the 2030 cost scenario (Figure S4). Even though battery storage will improve electrolyzer utilization beyond what is possible with PV alone (~30%; Figure S12), it is orders of magnitude more expensive (on a per-kilogram H_2 stored basis) than the estimated cost of pressure vessel H_2 storage for the 2030 scenario. For example, a battery storage capital cost of $350/kWh is approximately equal to $11665/kg of H_2 stored, not accounting for losses in storage and H_2 production. This makes it less valuable to deploy battery storage even when it can time-shift some or all of the curtailed PV generation and improve electrolyzer utilization. A small amount of battery storage is deployed in the most expensive H_2 storage scenario evaluated here, corresponding to the 2020 costs with pressure vessel H_2 storage (Figure S4).

In general, differences in average PV capacity factor explain lesser of the spatial variability in H_2 storage requirements than the variability in installed PV capacity and relative electrolyzer size, as noted in the coefficient of determination (R^2) values in Figure 2D. For example, even among the top PV resource sites (capacity factor $\geq$ 25%, 128 sites), the H_2 storage requirements differ by a factor of 2.5 for both storage types considered in Figure 2. Regions with a greater difference in PV availability between summer and winter months require increased H_2 storage capacity compared with regions with smaller seasonal variations in PV availability (Figure S5). Figure 3 illustrates the use of H_2 storage to manage diurnal and daily variations in PV availability and realize near-steady H_2 production flow (Figures 3C and 3D, product flow) for a hypothetical facility located in El Paso, TX.

Figure 4 shows the spatial distribution in levelized H_2 costs in the 2030 cost scenario with pressure vessel H_2 storage, with the highest costs ($11.8/kg) and lowest costs ($2.3/kg) observed in the United States northwest and southwest regions, respectively. Similar spatial trends are observed for the 2030 cost scenario with geological

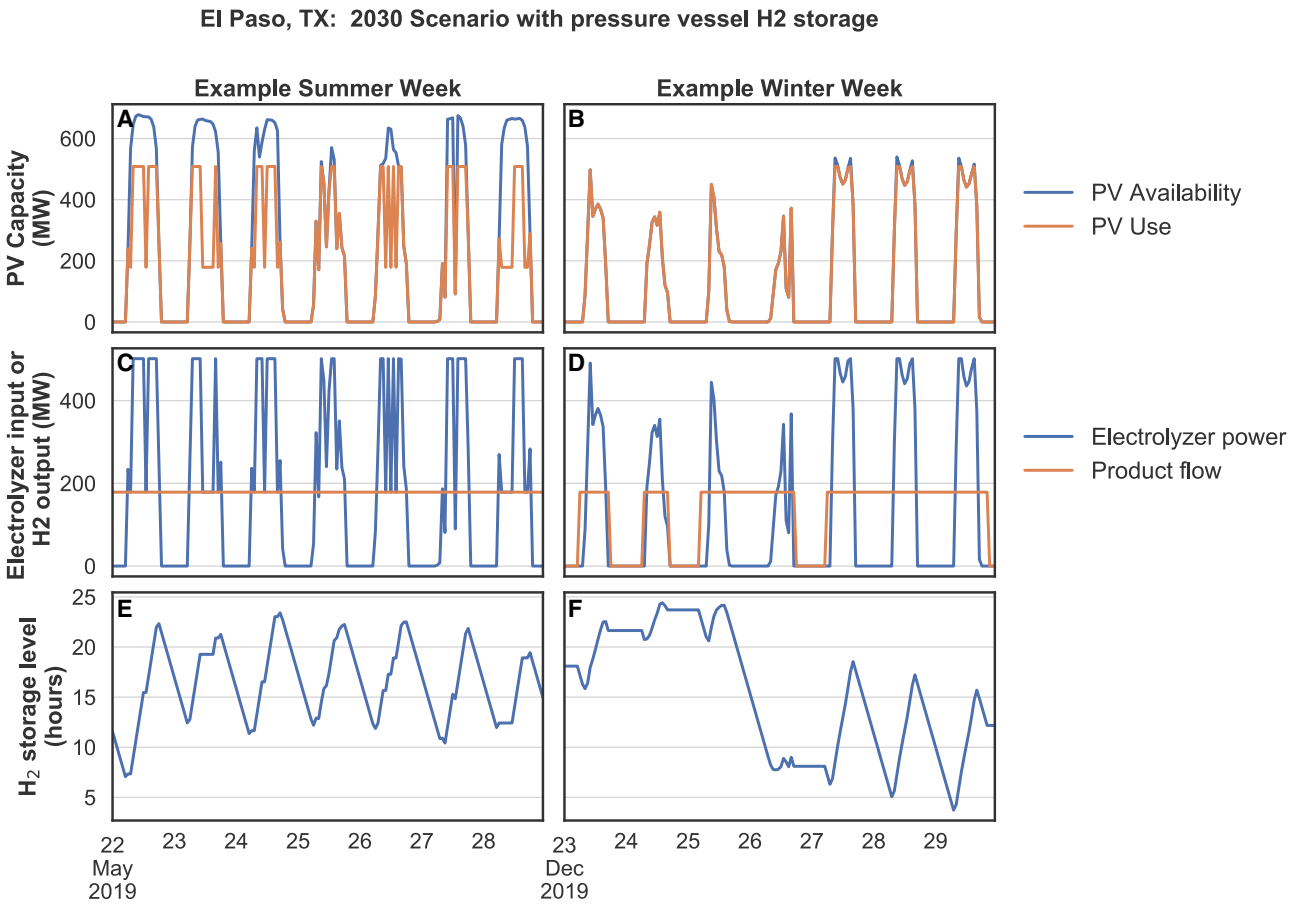

Figure 3. Illustration of Modeled Hourly Operations of a PV-Electrolysis H_2 Production Facility Located in El Paso, TX

(A–F) Average PV capacity factor = 25.9%. Operations are shown for a typical week in the summer (left) and winter (right). Shown are operational trends in PV (A and B), electrolyzer (C and D), and H_2 storage levels (E and F). The modeled facility is designed to produce 4.17 tonnes H_2/h (100 tons/day, with 10% hourly tolerance) and 95% annual plant availability. The time units used for displaying H_2 storage are estimated by dividing the hourly inventory of stored H_2 (in kilograms) with the nominal design flow rate of 4.17 tonnes H_2/h. The results shown correspond to the 2030 cost scenario with pressure vessel H_2 storage defined in Table 1.

H_2 storage, although the range of levelized costs is much smaller ($1.9–$4.2/kg) than the range of costs for the 2030 scenario with pressure vessel H_2 storage (Figure S6). Notably, the much lower cost of geological H_2 storage allows smoothening the temporal variations in PV availability at relatively low cost and leads to the average PV capacity factor being a strong indicator for levelized H_2 costs (R^2 value of 0.95 in Figure 2B). For the 2020 cost scenario, the spatial distribution in levelized H_2 costs is similar to the 2030 cost scenario, although the range of levelized costs is much higher ($5.7–$23.7/kg for pressure vessel H_2 storage [Figure S1] and $5.1– $11.4/kg and geological H_2 storage), indicating that the PV-electrolysis process shown in Figure 1 is currently not economically competitive with NG-based H_2 production routes.

Although the process shown in Figure 1 may not ever be an economically viable H_2 production pathway for low-quality PV resource regions like the United States northwest even in the 2030 cost scenario, there are 34 sites, mostly in the United States southwest and west Texas, with costs less than or equal to $2.5/kg and 245 sites with costs less than $3/kg while using pressure vessel H_2 storage. If geological H_2 storage is widely available, which we have not evaluated here, then many more

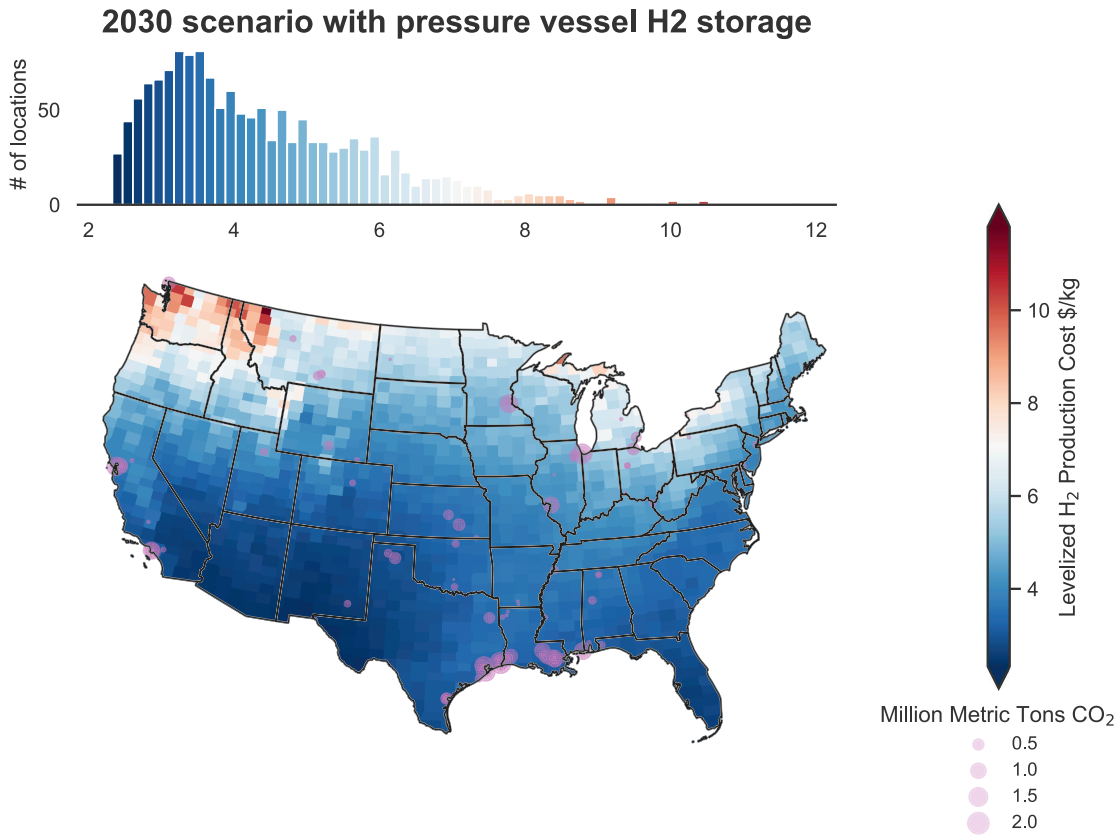

Figure 4. Costs of Continuous H_2 Supply via PV-Electrolysis +Pressure Vessel H_2 Storage for the 2030 Scenario in the Continental United States
The visualization is based on defining Voronoi polygons (Note S3) from costs estimated at 1,487 grid points using the integrated design and optimization model. PV resources in each location were characterized by TMY insolation data from the NREL Solar Radiation Database.[57] Pink markers indicate the location of existing H_2 production facilities according to the 2017 edition of the EPA GHG reporting program,[52] with the size of the marker proportional to annual GHG emissions attributed to H_2 production at the facility in 2017.

locations (621 of 1,487 locations) could meet the $2.5/kg cost threshold (Figure S6). Moreover, Figure 4 suggests that few low-cost regions, such as the Texas Gulf Coast and southern California, are also places with existing H_2 demand, as inferred by the presence of fossil fuel H_2 production facilities, making them attractive locations for practical deployment.

Figure 5 shows the breakdown of levelized H_2 costs for the 2030 scenario for 10 sites that have the highest average PV capacity factor among locations with existing fossil fuel-based H_2 production. Collectively, these sites accounted for 11.2 million tonnes of CO_2 equivalents per year or 25% of the GHG emissions associated with H_2 production in 2017 (Table S6). Because H_2 production sites are typically located close to the point of industrial consumption, these sites are promising locations for initial deployment of the PV-electrolytic H_2 process being studied here. Unsurprisingly, PV and electrolysis capital and fixed operating and maintenance (FOM) costs dominate the levelized cost across all the 10 locations, with PV costs alone accounting for between 61%–62% of total costs. Electrolyzer capital costs represent a smaller share of total costs because of their lower capital costs on a dollar per kilowatt basis versus PV and the oversizing of PV capacity relative to the electrolyzer capacity. Electrolyzer FOM costs, which include the estimated cost of periodical stack replacement (Note S2) contribute 11% of total costs across the locations. Compared with electrolyzer and PV costs, the cost of H_2 storage is a

Please cite this article in press as: Mallapragada et al., Can Industrial-Scale Solar Hydrogen Supplied from Commodity Technologies Be Cost Competitive by 2030?, Cell Reports Physical Science (2020), https://doi.org/10.1016/j.xcrp.2020.100174

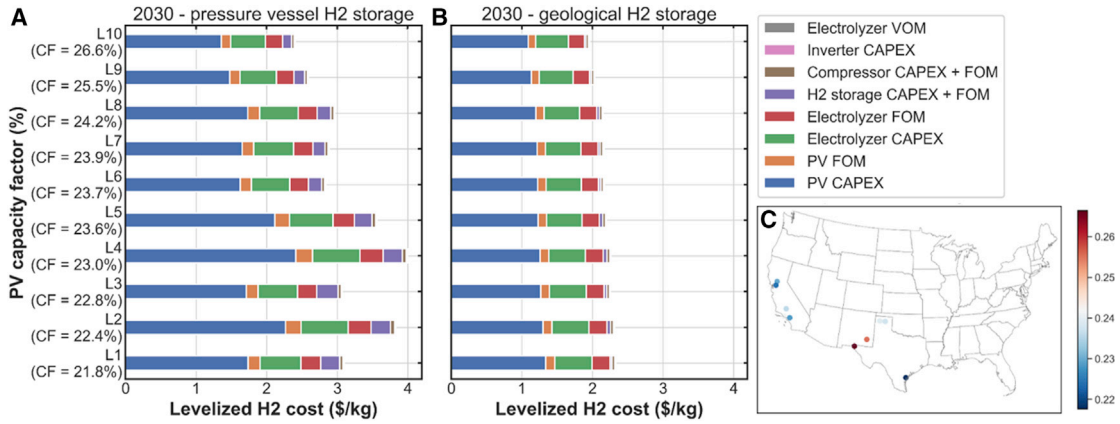

Figure 5. Levelized H_2 Cost Breakdown at 10 Favorable Sites for Near-Term Deployment for the 2030 Cost Scenario

(A and B) Breakdown of levelized H_2 costs for the 2030 scenario with pressure vessel H_2 storage (A) and geological H_2 storage (B), as defined in Table 1, at 10 potential sites that have the highest PV capacity factor among locations with existing fossil fuel-based H_2 production.

(C) Map of the locations, with color markers indicating differences in average PV capacity factor for the evaluated locations.

In (A) and (B), the costs of the inverter and electrolyzer are not visible because their contributions are relatively minor compared with the x axis scale. PV availability was characterized using TMY insolation data from the National Solar Radiation Database.[37] VOM, variable operating and maintenance; FOM, fixed operating and maintenance; capex, installed capital costs; CF, average PV capacity factor.

relatively minor share of total costs even when using the more expensive H_2 storage option of pressure vessels. The costs of the inverter, H_2 compression, and feed water costs (Figure 5, electrolyzer variable operating and maintenance [VOM]) contribute a relatively minor share of overall costs and are therefore not considered for further sensitivity analysis.

Effect of Inter-annual Variations in PV Resources

The estimated design trends and levelized costs discussed above are based on characterizing PV resources for each hour of the year using TMY insolation data, which are synthesized from multiple years of data and are commonly used to represent typical variability in PV resources in VRE-related design studies. Here we investigate the reliability of the resulting plant design to accommodate "atypical" variations in PV availability, such as inter-annual variability,[49] by simulating their operation over 20 years using historical PV resource data for 1998–2017. For this, we solved the design optimization model for each location and a specified cost scenario while fixing all sizing decisions to be equal to values identified from solving the model with TMY PV resource data. Figure 6 highlights the annual availability factor of TMY-based plant designs at 10 locations when simulated with PV resource data from historical weather years (1998–2017). Although inter-annual variations in PV availability result in less than a 95% annual availability factor for some years, the overall variation in annual availability is relatively narrow, with a lowest annual availability factor of 90%. Moreover, the number of hours of lost production (i.e., when plant output is below the design flow rate) is in the range of 5%–11% (Figure S7). Similar trends are observed in the case of a TMY-based plant design using geological H_2 storage (see Figure S8). These comparisons indicate that designs obtained using TMY data could yield a reasonably steady supply of H_2 even with inter-annual variations in PV availability and, thus, may be acceptable for a screening analysis to explore promising locations and general system design heuristics (e.g., an electrolyzer-to-PV ratio of less than 1). That said, use of multiple years of historical PV availability may be important for optimizing detailed plant design at a specific location.

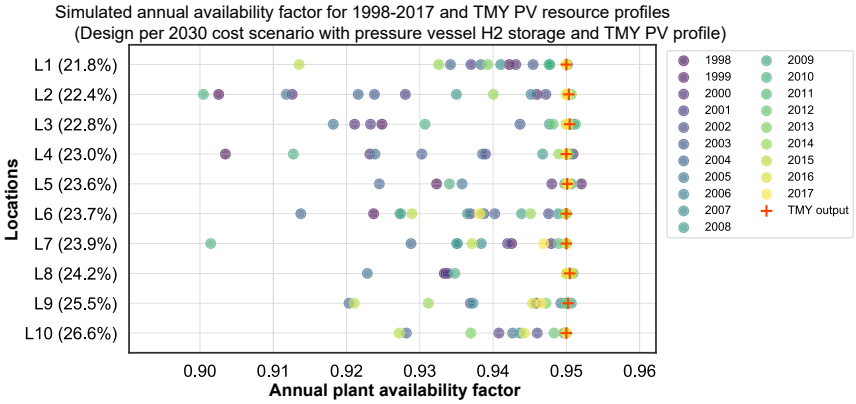

Figure 6. Effect of Inter-annual PV Variability on Annual Availability of H_2 Supply for TMY-Based Plant Designs

Shown is the annual plant availability factor for a H_2 production facility, sized using solar resource characterized via typical meteorological year (TMY) data, but simulated with historical PV resource availability profiles for 1998–2017 (colored circles). Plant availability factor is defined as the ratio of total annual H_2 production of the facility for each weather year (historical or TMY) relative to the design amount (after derating for maximum allowed variation in the hourly flow rate of 10%). Results are shown for 10 locations, identified in Figure 5, for the 2030 cost scenario with pressure vessel H_2 storage, as defined in Table 1.

Effect of Electrolyzer and H_2 Storage Cost and Performance

The results from the 2030 cost scenario analysis indicate a potential for numerous United States sites to produce H_2 via the process shown in Figure 1 at costs of $2.5/kg or lower. However, there is considerable uncertainty regarding the cost and performance of individual components, particularly electrolysis and H_2 storage. Here we further explore the effect of component cost and performance as well as system design parameters on the cost competitiveness of electrolytic H_2 production at the 10 promising sites identified for initial deployment in Figure 5. The findings from sensitivity analyses at these 10 sites are meant to be illustrative of the possible outcomes at other similar resource quality locations in the United States, identified in the previous section. Given the relative immaturity of PEM electrolysis or H_2 storage compared with PV, we focus our analysis on the costs and performance of the former two technologies while keeping PV costs constant at the values assumed for 2030 ($500/kW DC).

Figure 7 highlights the combination of electrolyzer capital costs, FOM costs, energy efficiency, and H_2 storage capital costs that lead to levelized costs of $2.5/kg or lower while holding PV capital and FOM costs constant at $500/kW DC and 1% of capital costs, respectively. The values for the remaining model input parameters used in Figure 7 correspond to the 2030 scenario defined in Table 1 and Table S4.

A central finding of Figure 7 is the effect of H_2 storage costs on the magnitude of electrolyzer capital cost reductions needed to achieve levelized H_2 costs of $2.5/kg or less. This is indicated by the fewer number of green versus blue markers in each panel of Figure 7. The typical scale of geological H_2 storage, on the order of thousands of tonnes, overlaps with the storage capacity estimated for the process configurations highlighted in Figure 7. However, geological H_2 storage may be limited in its geographic availability, in which case further electrolyzer cost reductions are needed to offset the relatively high cost of pressure vessel H_2 storage. For instance, at the best PV resource location, L10, and an electrolyzer efficiency of 70%, Figure 7 highlights that achieving $2.5/kg or lower levelized costs with

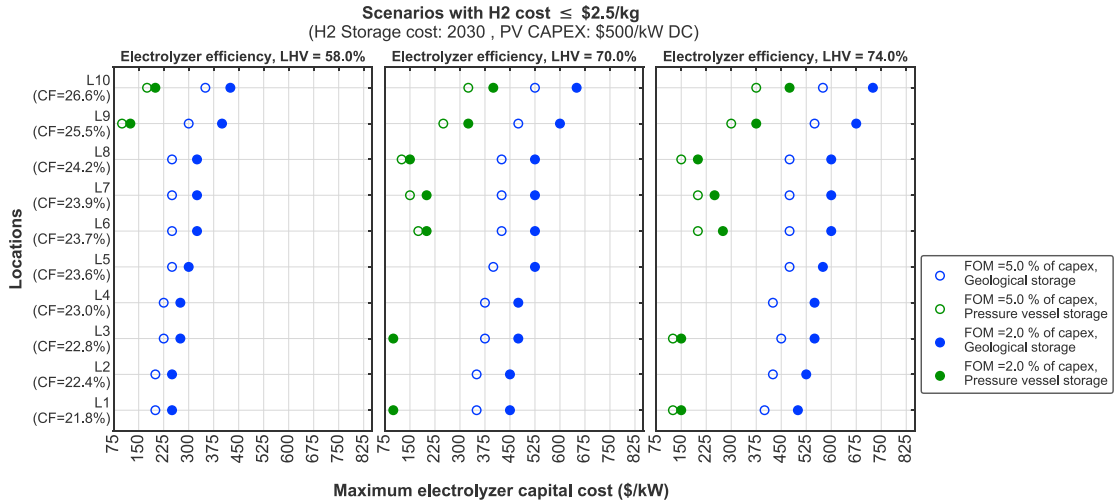

Figure 7. Combination of Locations, Electrolyzer Cost and Performance, and H_2 Storage Costs that Result in Levelized Costs ≤$2.5/kg

Parameters varied, including electrolyzer capital costs, FOM costs, energy efficiency (based on lower heating value [LHV]), and H_2 storage capital costs. The cost of geological and pressure vessel H_2 storage are equal to $3/kg and $345/kg, respectively, corresponding to the 2030 cost scenario. The costs of the remaining parameters are defined under the "2030" column in Tables 1 and S4. For each location, points are only marked for combinations of parameter values that result in costs of $2.5/kg or lower. Filled and empty circles correspond to FOM costs equal to 2% and 5% of capital costs, respectively.

pressure vessel H_2 storage and geological H_2 storage requires electrolyzer capital cost reductions (compared with 2020 costs of $800/kW) in the range of 50%–59% and 18%–34%, respectively. As a reference, electrolyzer capital costs are estimated to have declined by 3%–7% per year during 2003–2016.[29] Although a $2.5/kg levelized cost threshold excludes the option of pressure vessel H_2 storage in 8 of the 10 sites in Figure 7 for the plausible 2030 scenario of electrolyzer cost and performance (capital cost of $300/kW and 70% efficiency), a threshold cost of $3/kg makes the system with pressure vessel H_2 storage feasible at 7 of 10 sites (Figure S9). Additionally, $3/kg or lower levelized H_2 costs with pressure vessel H_2 storage appear to be feasible at multiple locations with 2030 electrolyzer cost and performance, even when the cost of pressure vessel storage remains the same as the 2020 estimates (Figure S10). Similarly, for geological H_2 storage, $2.5/kg or lower levelized H_2 costs are achievable at 8 of the 10 sites with 2030 electrolyzer costs and performance and 2020 H_2 storage costs (Figure S11).

A comparison of the filled and unfilled markers of the same color in Figure 7 highlights the effect of decreasing electrolyzer FOM costs on levelized H_2 costs. As modeled here, FOM costs include the annualized cost of stack replacement, and this cost is expected to decrease as stack lifetimes increase.[47,50] Figure 7 suggests that scenarios with high FOM costs (5% of installed capital costs [capex]) and geological storage (blue unfilled markers) lead to higher threshold values for electrolyzer capital costs (or lower levelized costs) compared with scenarios with low FOM costs (2% capex) and pressure vessel storage (green filled markers). This finding suggests that levelized costs are more sensitive to the type of H_2 storage compared with electrolyzer FOM costs.

The effect of increasing electrolyzer efficiency increases the number of combinations of electrolyzer costs, storage type, and locations that can achieve less than $2.5/kg levelized H_2 costs (Figure 7, 24 markers in the left panel versus 32 markers in the center panel and 34 markers in the right panel). Based on the difference in maximum

electrolyzer capital cost across the panels in Figure 7, one can evaluate threshold cost increases associated with efficiency improvements that still result in levelized costs of $2.5/kg or less. For example, with geological H_2 storage and FOM costs equal to 5% of capex, approaches that improve efficiency from 70% to 74% without increasing capital costs more than $50–$75/kW will be able to achieve levelized costs below $2.5/kg at the 10 locations. Conversely, if electrolyzer efficiencies remain at their current levels of 58%, then electrolyzer capital costs will have to be in the range of $200–$350/kW to achieve levelized costs of $2.5/kg or less at the 10 locations (Figure 7, left panel). Finally, this analysis assumes the electrolyzer energy efficiency to be independent of the device's power loading, whereas in practice, the system efficiency generally decreases with increasing loading levels because of resistive losses.[28,36] For the process shown in Figure 1, however, the electrolyzer hourly loading is predominated by two states, at or near full operation or zero output (Figure S12). Consequently, the approximation of constant electrolyzer efficiency across loading levels has a relatively small effect on system design and cost outcomes (Figure S13).

Effect of System Factors

Although several studies of electrolytic H_2 production assume the annual plant availability to be the same as the PV capacity factor,[14,28,29] our analysis defines it as an independent parameter. In general, increasing plant availability above the average PV capacity factor necessitates the need for additional energy storage and/or overbuilding PV capacity, both of which increase levelized costs. When H_2 storage is cheap, as in the case of geological H_2 storage, it is more cost-effective to increase H_2 storage capacity than overbuild PV capacity, whereas the opposite is true in case of higher H_2 storage costs corresponding to pressure vessel H_2 storage (Figures S14–S16). Figure 8 shows that plant availability requirements have a significant effect on levelized H_2 costs when considering more expensive pressure vessel H_2 storage. For instance, as plant availability is changed from 100% to 70%, the levelized costs for the highest PV capacity factor site, L10, decrease by nearly $1/kg in the case of pressure vessel H_2 storage compared with less than $0.2/kg in the case of underground H_2 storage. When contemplating H_2 infrastructure requirements to meet spatially distributed H_2 demand, the above finding suggests that it may be cost-effective to operate facilities with access to geological H_2 storage at or near 100% availability to compensate for the lower availability in H_2 supply from other facilities using pressure vessel H_2 storage (that may be located to closer to demand).

Because the levelized cost is nearly entirely made up by capital costs, the assumed cost of capital is a key determinant of system costs. Figure S17 quantifies the sensitivity of the levelized costs to differing assumptions regarding the cost of capital, which is used to evaluate the fraction of total capital costs included in the annualized cost calculations (via the capital charge factor; Table S4). Across the locations and storage costs, changing cost of capital from the default value of 8.1% to 12% or 5% results in an increase or decrease in costs by roughly $0.5–1/kg. The costs of H_2 at the highest PV resource sites show the smallest change with changing cost of capital because of the relatively small installed PV capacity, which dominates levelized costs (Figures 5A and 5B).

Comparison with NG Pathways for the 2030 Scenario

Currently, NG SMR without CCS is the most economical pathway for H_2 production in the United States, with an estimated cost near $1/kg of H_2 for centralized production (around 300 tonnes/day).[26,39,40] Therefore, in the absence of any policy incentive (e.g., carbon price) for low-carbon H_2 production, there is no economic driver

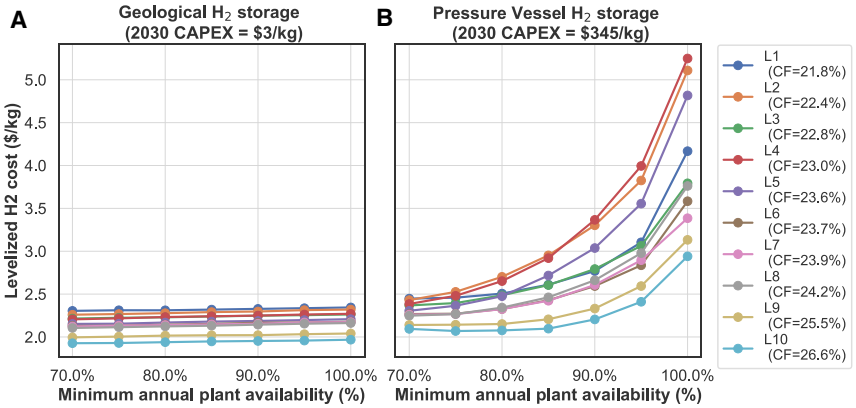

Figure 8. Effect of Annual Plant Availability Requirements on Levelized H_2 Costs

Shown is the sensitivity of levelized H_2 production costs to changes in minimum plant availability requirements for different H_2 storage capital costs and at various locations in the United States. Location labels, L1–L10, refer to the locations with the same name defined in Figure 5. Aside from storage capital costs, costs of other input parameters correspond to the 2030 scenario defined in Tables 1 and S4. Hourly H_2 production requirements held constant at 4.17 tonnes/h (with 10% hourly tolerance) across the differing plant availability requirement cases.

to deploy the PV-electrolysis process shown in Figure 1, even for the range of future technology costs and performance scenarios investigated above. The NG SMR process is associated with life cycle GHG emissions of 10–17 kg CO_2 equivalents/kg H_2,[39,40] of which process GHG emissions account for approximately 9 kg CO_2/kg H_2,[51] whereas the remaining emissions result from upstream activities (NG production, processing, and transmission). Figure 9 shows the estimated costs of avoiding process CO_2 emissions from NG SMR by substituting with H_2 produced from the process shown in Figure 1 for the 2030 scenario at the top 10 PV resource locations with existing NG-based H_2 production. These costs, referred as avoided CO_2 costs, are estimated as the ratio of the difference in levelized costs to the difference in CO_2 emission intensity between the two processes (Equation 1), where NG SMR is characterized with a cost of $1.15/kg and 9.28 kg CO_2/kg H_2.[26]

$$Avoided\ \ CO_2\ \ cost = \frac{LevelizedCost_{PV-Electrolysis} - LevelizedCost_{NG-SMR}}{EmissionIntensity_{NG-SMR} - EmissionIntensity_{PV-Electrolysis}} \quad \text{(Equation 1)}$$

For 2030 electrolyzer cost and performance (defined in Table 1), the avoided CO_2 costs for 6 of the 10 sites (L3 and L6–L10) in Figure 7, which collectively accounted for 14.5% of H_2-related GHG emissions in 2017 (Table S6)[52] is in the range of $87–$120/ton CO_2 with geological H_2 storage and $135–$207/ton CO_2 with pressure vessel H_2 storage. The range of avoided CO_2 costs for PV-electrolysis plus geological H_2 storage overlaps well with the range of avoided CO_2 costs (including cost of capture, transport, and storage) for NG-based H_2 with CCS based on SMR or ATR approaches ($77–$115 ton/CO_2[6,39,40]). Despite the cost of CO_2 capture being slightly less for an ATR plant than an SMR plant, the choice of reforming technology has a relatively minor effect on the total avoided CO_2 costs for NG-based H_2 production[6,40,42] and, consequently, on the comparison with PV-electrolytic H_2. The avoided CO_2 costs can be recovered in markets with incentives for fuel emission intensity reduction, such as the LCFS program in California, to achieve cost parity against more CO_2-emitting but cheaper cost pathways, like NG SMR without CCS. The average monthly price of emission credits generated via the LCFS program, which is capped at $200/tonne CO_2, has ranged from $122/tonne CO_2 to

Please cite this article in press as: Mallapragada et al., Can Industrial-Scale Solar Hydrogen Supplied from Commodity Technologies Be Cost Competitive by 2030?, Cell Reports Physical Science (2020), https://doi.org/10.1016/j.xcrp.2020.100174

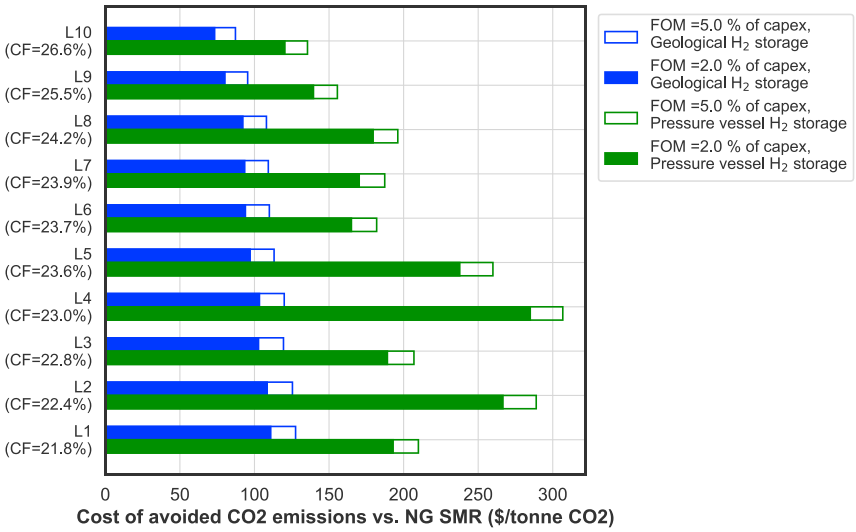

Figure 9. Avoided CO_2 Cost for H_2 Produced from PV-Electrolysis with Storage versus NG SMR

Shown are CO_2 avoided costs estimated based on the NG-SMR levelized cost of $1.15/kg (2016 United States dollars)[22] and process emissions of 9.28 kg CO_2/kg H_2.[49] The results are based on the 2030 scenario defined in Tables 1 and S4. Capital cost of pressure vessel and geological H_2 storage correspond to $345/kg and $3/kg, respectively. Location labels, L1–L10, refer to the locations with the same name defined in Figure 5. Hourly H_2 production requirements held constant at 4.17 tonnes/h (with 10% tolerance) and 95% annual availability.

$190/tonne CO_2 over the period of March 2018–February 2019.[53] This range overlaps with the range of avoided CO_2 costs estimated here.

The avoided CO_2 costs estimated here will likely be lower when calculated based on avoided life cycle GHG emissions instead of process GHG emissions because of higher upstream GHG emissions associated with NG-based H_2 compared with PV-electrolytic H_2.[39] For example, according to Parkinson et al.,[39] the central estimate for life cycle GHG emissions for H_2 produced from NG SMR and PV-electrolysis is 13.2 kg CO_2 equivalents/kg H_2 and 2.2 kg CO_2 equivalents/kg H_2, respectively. Using these life cycle GHG emissions rather than process-based GHG emissions in the avoided CO_2 cost calculations of Equation 1 lowers the avoided CO_2 cost for PV-electrolysis with either H_2 storage option for 6 of the 10 locations (L3 and L6–L10) by ~16% ($74–$100/tonne CO_2 for geological H_2 storage and $114–$174/tonne CO_2 for pressure vessel H_2 storage).

Although the design and cost outcomes presented here for PV-electrolysis correspond to a scale of 100 tons of H_2/day, many of the system components, with the exception of the H_2 compressor (which has a relatively small contribution to total costs; Figure 5), are modular in nature above a certain scale. This implies that the levelized costs are likely to be similar if the scale of production was changed, say, to serve distributed H_2 demand from a collection of H_2 fuel cell vehicle refueling stations (1–2 tonnes/day). For these end uses, PV-electrolysis coupled with pressure vessel H_2 storage could potentially be deployed closer to demand (i.e., refueling stations) to minimize H_2 transportation costs. Low-carbon H_2 supply with NG pathways at distributed scale has yet to be demonstrated, and centralized routes will be associated with additional delivery costs which, when completed via dedicated H_2 pipelines, are estimated to be around $2/kg H_2.[27] Consequently, the delivered cost of H_2 from NG SMR coupled with pipeline transport for distributed end uses could be as

high as $3/kg, not accounting for the cost of CCS. This implies that PV-electrolysis coupled with pressure vessel H_2 storage could potentially also be a cost-competitive supply option for distributed end uses at the highest PV resource locations if the 2030 cost scenario is realized.

DISCUSSION

Using plausible projections of 2030 costs and performance of commodity technologies for PV, electrolysis, and H_2 storage, we identify a set of sunny United States locations and plant configurations that could supply industrial-scale quantities of H_2 round-the-clock at costs at or below $2.5/kg H_2.

The majority of the instances identified with a cost of $2.5/kg or less are contingent on (1) a reduction in electrolyzer capital costs between 28% and 62% compared with current costs for multi-megawatt systems depending on the case; (2) ~20%–28% improvements in electrolyzer efficiency beyond current levels; (3) availability of geological H_2 storage, which not only enables low H_2 storage costs but could also provide sufficient storage capacity to support supply for industrial H_2 demand; and (4) PV capital costs of $500/kW DC, which seems plausible given historical trends and available projections.[12,43,44] Moreover, under these conditions, PV-electrolysis coupled with H_2 storage at select locations could displace NG-based H_2 supply with costs of avoiding process CO_2 emissions similar to costs estimated for deploying CCS at NG SMR facilities. These findings are made possible by the integrated design approach used in this study; notably, the costs would be considerably higher if one used the same technology cost and performance assumptions but did not optimize an individual component's size (e.g., electrolyzer to PV ratio < 1) at each location. Our approach not only quantifies the levelized cost effects associated with choices inherent in electrolyzer design, such as increasing efficiency versus decreasing capital costs, but also compares them with changes in costs and performance of other equipment; namely, the costs of PV and energy storage.

Estimates of future production costs are always uncertain. How might different assumptions change our conclusions? Factors that might lead to an under-estimate of costs include (1) a less than anticipated decline in the cost of individual technologies by 2030, notably electrolyzer and PV; (2) the potential cost savings from DC-DC integration of electrolyzer and PV systems being outweighed by the practicality and reduced performance of coupled operation; and (3) limitations regarding land availability and/or geological H_2 storage at the best sites, perhaps based on safety concerns about H_2 storage. Factors that might lead to an over-estimate of costs include our neglect of wind power and the benefits of the negative correlation between wind and solar availability in providing low-carbon power with higher availability than PV systems alone. The higher-capacity factor of wind as well as high resource availability in regions with low-quality solar resources (e.g., the United States Midwest) makes a compelling case for studying the economics of wind-based electrolytic H_2 production integrated with on-site storage. We neglected the benefits of grid integration, which could lower costs at the expense of increasing GHG emission intensity. Potential economic benefits of grid integration include providing ancillary services via electrolyzer operation, reducing the installed on-site capacity of renewable generation, electrolyzer and H_2 storage, as well as exporting any excess renewable electricity. The GHG emission effects of complete reliance on grid electricity for electrolysis, however, could be significant in the near term. For example, in California, renewables, including wind and solar, accounted for 29% of total generation in 2017,[54] leading to an average CO_2 emission intensity of electricity generation in

2017 of 212 kg CO_2/MWh.[55] This translates into CO_2 emissions of around 10 tonnes CO_2 per ton H_2 using a 70% electrolyzer efficiency, which is similar to the life cycle CO_2 emission intensity of H_2 produced from NG SMR. We neglected the use of curtailed PV electricity for consumption within the industrial plant that is also consuming the produced H_2. This approach could reduce electricity demand from the grid or onsite fossil-based generation, which reduces electricity supply costs for industrial application while also lowering plant direct and/or indirect CO_2 emissions. Finally, we only examined the United States, but the PV-electrolytic H_2 system may be even more cost effective in other regions with higher quality solar resources, such as Chile and India, regions with rapidly growing energy demands.

Our estimates of levelized H_2 cost and avoided CO_2 costs ignore the effect of existing policies supporting low-carbon H_2 or fuel production. As noted earlier, existing policies supporting renewable energy, like the LCFS and modified accelerated cost recovery system in the United States available for PV,[56] could further improve the cost effectiveness of dedicated PV-based electrolytic H_2. Such policies could also reduce the costs of competing H_2 supply technologies, such as NG SMR or ATR with CCS, so the effect on carbon-avoided costs is less clear.

Explicit treatment of the variability of PV output on timescales from hours to years is needed to understand the optimal system design and resulting H_2 production costs. In the analysis for the 2030 scenario with pressure vessel H_2 storage spanning nearly 1,500 locations, for example, the average PV capacity factor explains 61%, 61%, 58%, and 55% of the variation observed in, respectively, the H_2 production cost, installed PV capacity, relative electrolyzer size, and duration of installed H_2 storage capacity. Moreover, these values are based on characterizing annual PV resources at an hourly resolution using TMY data, but our simulations of plant availability using PV resource from individual years suggest that use of longer historical time series (or more judiciously selected annual time series) could be important to minimize costs in the practical design of high-availability, VRE-based H_2 production systems.

Future work could re-assess the promising sites identified for H_2 production in this study after factoring in the historical inter-annual variability in PV resources as well as the potential for geological H_2 storage sites and their various attributes (e.g., formation pressure, cushion gas requirements[18]). Further analysis is also needed to estimate the total potential supply of H_2 at each site that considers land availability constraints (e.g., excluding urban areas and preservation lands), manufacturing supply chain considerations, as well as the cost of importing H_2 from neighboring locations.

Previous attempts to expand the role of H_2 across the economy generally focused on transportation as the initial-use case. Instead, we argue for expanding use of H_2 in the industrial sector as a way to rapidly scale up electrolysis technologies and kickstart sectoral emission reduction efforts by 2030 to be consistent with mid-century deep decarbonization goals. Under a strong climate policy, our analysis suggests that electrolytic production of H_2 integrated with large solar PV arrays could, in areas of good solar resources, be cost competitive as an industrial feedstock by 2030.

EXPERIMENTAL PROCEDURES

Resource Availability

Lead Contact

Further information and requests for resources should be directed to the Lead Contact, Dharik Mallapragada (dharik@mit.edu).

Materials Availability

All of the data and methods used, including optimization models, are available from the Lead Contact upon reasonable request.

Data and Code Availability

The parameter inputs to characterize cost and performance technologies are documented in the study, with the exception of PV resource availability, which is drawn from a publicly available data source.[57] The scripts used to perform the modeling and a complete sample dataset are available at https://www.dropbox.com/sh/ros1svyybw09xhz/AADEajd-LPhYqRKeLOpDNYZAa?dl=0.

Modeling Approach and Data Inputs

We use an integrated design and operations optimization model to evaluate the levelized cost of H_2 production across the continental United States. The model determines the cost-optimal size and hourly operation of all components throughout the year in the process shown in Figure 1 to meet the specified hourly H_2 production requirements while minimizing total annualized capital and operating costs. The model includes the following constraints associated with hourly plant operation: (1) inter-temporal constraints governing energy storage (H_2, battery) operation; (2) hourly limits on PV resource availability; (3) for each component, hourly power flows cannot exceed the installed power capacity; (4) throughput-based energy requirements for H_2 compression prior to storage; (5) minimum downtime requirements for the entire plant (12 h), and (6) annual plant availability requirements.

The model makes the following assumptions about individual component operation: (1) constant specific power consumption for the electrolyzer and compressor irrespective of loading; (2) fully flexible operation of the electrolyzer, compressor, H_2 storage, and battery energy storage, implying that each component can go from zero to the maximum power rating within an hour; (3) no minimum stable operating level for the electrolyzer; and (4) no minimum state of charge requirements for H_2 or battery storage. A complete mathematical description of the optimization model is available in Note S1. Unless stated otherwise, all results correspond to solutions where the optimization model was terminated with a 1% or lower optimality gap.

Annual hourly PV capacity factor data for the various United States locations evaluated was derived using TMY insolation data available from the National Solar Radiation Database (NSRDB)[57] in conjunction with the pvlib simulation toolbox.[58] The pvlib simulation toolbox[58] converts the insolation time series into a capacity factor time series (DC values) based on a pre-specified PV system configuration, which, in this analysis, is assumed to be a single-axis tracking system that is oriented horizontally. The cost and performance assumptions used to characterize operating and capital costs of various components across the 2020 and 2030 scenarios is summarized in Table 1 and Table S4.

The spatial distribution of levelized H_2 production costs shown in Figures 2 and 4 was developed based on evaluating the optimization model for 1,487 locations across the United States. These locations correspond to points on a grid developed from evenly spaced latitudes and longitudes spanning the continental United States land area. The levelized H_2 production costs estimated for the 1,487 locations were translated into a smooth color map for the continental United States using a Voronoi diagram (Note S3).

SUPPLEMENTAL INFORMATION

Supplemental Information can be found online at https://doi.org/10.1016/j.xcrp.2020.100174.

ACKNOWLEDGMENTS

The authors acknowledge the input of Abhishek Bose at Massachusetts Institute of Technology (MIT) Energy Initiative for help with evaluation of the optimization model. D.S.M. and P.I. acknowledge funding support from the Low-Carbon Energy Center on Electric Power Systems at the MIT Energy Initiative. E.G. acknowledges funding support from the Low-Carbon Energy Center on Carbon Capture, Utilization, and Storage at the MIT Energy Initiative.

AUTHOR CONTRIBUTIONS

Conceptualization, D.W.K., D.S.M., E.G., and F.M.O.; Methodology, D.S.M. and E.G.; Investigation, D.S.M., E.G., and P.I.; Writing—Original Draft, D.S.M.; Visualization, D.S.M. and P.I.; Project Administration and Funding Acquisition, D.W.K., D.S.M., and F.M.O.

DECLARATION OF INTERESTS

F.M.O. is Senior Vice President for Strategy at Orsted Onshore North America, a developer and owner of wind and solar projects in the United States. D.W.K. is a founder and board member of Carbon Engineering, a developer of direct air capture technologies that might be used to produce fuels using solar hydrogen as an input.

Received: September 23, 2019
Revised: June 3, 2020
Accepted: July 23, 2020
Published: August 19, 2020

REFERENCES

1. U.S. Energy Information Administration (2019). Annual Energy Outlook 2019: with projections to 2050. https://www.eia.gov/outlooks/aeo/pdf/aeo2019.pdf.
2. Balcombe, P., Brierley, J., Lewis, C., Skatvedt, L., Speirs, J., Hawkes, A., and Staffell, I. (2019). How to decarbonise international shipping: Options for fuels, technologies and policies. Energy Convers. Manag. *182*, 72–88.
3. Schäfer, A.W., Barrett, S.R.H., Doyme, K., Dray, L.M., Gnadt, A.R., Self, R., O'Sullivan, A., Synodinos, A.P., and Torija, A.J. (2019). Technological, economic and environmental prospects of all-electric aircraft. Nat. Energy *4*, 160–166.
4. World Energy Council Netherlands (2018). Hydrogen- Industry as catalyst: Accelerating the decarbonisation of our economy to 2030. http://www.wereldenergieraad.nl/wp-content/uploads/2019/02/190207-WEC-brochure-2019-A4.pdf.
5. Davis, S.J., Lewis, N.S., Shaner, M., Aggarwal, S., Arent, D., Azevedo, I.L., Benson, S.M., Bradley, T., Brouwer, J., Chiang, Y.-M., et al. (2018). Net-zero emissions energy systems. Science *360*, eaas9793.
6. International Energy Agency (2019). The Future of Hydrogen: Seizing today's opportunities. https://www.iea.org/reports/the-future-of-hydrogen.
7. International Energy Agency (2020). Hydrogen Projects Database. https://www.iea.org/reports/hydrogen-projects-database.
8. IPCC (2018). Global Warming of 1.5°C. https://www.ipcc.ch/sr15/.
9. International Renewable Energy Agency (2019). Hydrogen: A Renewable Energy Perspective. https://www.irena.org/-/media/Files/IRENA/Agency/Publication/2019/Sep/IRENA_Hydrogen_2019.pdf.
10. Thema, M., Bauer, F., and Sterner, M. (2019). Power-to-Gas: Electrolysis and methanation status review. Renew. Sustain. Energy Rev. *112*, 775–787.
11. ITM Power (2019). Interim Results Presentation. https://www.itm-power.com/images/Investors/PresentationsAndResearch/Interim-Results-presentation_18.pdf.
12. Bloomberg New Energy Finance (2019). New Energy Outlook 2019. https://about.bnef.com/new-energy-outlook/.
13. National Renewable Energy Laboratory (2018). Annual Technology Baseline. https://atb.nrel.gov/electricity/2018/.
14. Shaner, M.R., Atwater, H.A., Lewis, N.S., and McFarland, E.W. (2016). A comparative technoeconomic analysis of renewable hydrogen production using solar energy. Energy Environ. Sci. *9*, 2354–2371.
15. Tietze, V., Luhr, S., and Stolten, D. (2016). Bulk Storage Vessels for Compressed and Liquid Hydrogen. In Hydrogen Science and Engineering: Materials, Processes, Systems and Technology, D. Stolten and B. Emonts, eds. (Wiley-VCH), pp. 659–690.
16. Air Products and Chemicals Inc. (2020). Typical Bulk Gas Storage Systems. http://www.airproducts.com/Products/Gases/supply-options/bulk-deliveries-and-storage-systems/typical-bulk-gas-storage-systems.aspx.
17. U.S. Department of Energy (2017). US DRIVE Hydrogen Delivery Technical Team Roadmap. https://www.energy.gov/eere/vehicles/downloads/us-drive-hydrogen-delivery-technical-team-roadmap.
18. Lord, A.S., Kobos, P.H., and Borns, D.J. (2014). Geologic storage of hydrogen: Scaling up to meet city transportation demands. Int. J. Hydrogen Energy *39*, 15570–15582.
19. Forsberg, C. (2006). Assessment of Nuclear-Hydrogen Synergies with Renewable Energy

Systems and Coal Liquefaction Processes (Oak Ridge National Laboratory).

20. Lord, A.S. (2009). Overview of Geologic Storage of Natural Gas with an Emphasis on Assessing the Feasibility of Storing Hydrogen (Sandia National Laboratories).

21. Sepulveda, N.A., Jenkins, J.D., de Sisternes, F.J., and Lester, R.K. (2018). The Role of Firm Low-Carbon Electricity Resources in Deep Decarbonization of Power Generation. Joule *2*, 2403–2420.

22. Denholm, P., O'Connell, M., Brinkman, G., and Jorgenson, J. (2015). Overgeneration from Solar Energy in California: A Field Guide to the Duck Chart (NREL).

23. Schoenung, S.M., and Keller, J.O. (2017). Commercial potential for renewable hydrogen in California. Int. J. Hydrogen Energy *42*, 13321–13328.

24. Ong, S., Campbell, C., Denholm, P., Margolis, R., and Heath, G. (2013). Land-Use Requirements for Solar Power Plants in the United States. (NREL).

25. Eurek, K., Sullivan, P., Gleason, M., Hettinger, D., Heimiller, D., and Lopez, A. (2017). An improved global wind resource estimate for integrated assessment models. Energy Econ. *64*, 552–567.

26. National Renewable Energy Laboratory (2018). H2A: Hydrogen Analysis Production Case Studies. https://www.nrel.gov/hydrogen/h2a-production-case-studies.html.

27. Ramsden, T., Ruth, M., Diakov, V., Laffen, M., and Timbario, T. (2013). Hydrogen Pathways: Updated Cost, Well-to-Wheels Energy Use, and Emissions for the Current Technology Status of Ten Hydrogen Production, Delivery, and Distribution Scenarios (National Renewable Energy Laboratory).

28. International Renewable Energy Agency (2018). Hydrogen from Renewable Power: Technology Outlook for the Energy Transition. https://www.irena.org/publications/2018/Sep/Hydrogen-from-renewable-power.

29. Glenk, G., and Reichelstein, S. (2019). Economics of converting renewable power to hydrogen. Nat. Energy *4*, 216–222.

30. Guerra, O.J., Eichman, J., Kurtz, J., and Hodge, B.M. (2019). Cost Competitiveness of Electrolytic Hydrogen. Joule *3*, 2425–2443.

31. Grüger, F., Hoch, O., Hartmann, J., Robinius, M., and Stolten, D. (2019). Optimized electrolyzer operation: Employing forecasts of wind energy availability, hydrogen demand, and electricity prices. Int. J. Hydrogen Energy *44*, 4387–4397.

32. Zhao, L., and Brouwer, J. (2015). Dynamic operation and feasibility study of a self-sustainable hydrogen fueling station using renewable energy sources. Int. J. Hydrogen Energy *40*, 3822–3837.

33. Hou, P., Enevoldsen, P., Eichman, J., Hu, W., Jacobson, M.Z., and Chen, Z. (2017). Optimizing investments in coupled offshore wind -electrolytic hydrogen storage systems in Denmark. J. Power Sources *359*, 186–197.

35. Gillessen, B., Heinrichs, H.U., Stenzel, P., and Linssen, J. (2017). Hybridization strategies of power-to-gas systems and battery storage using renewable energy. Int. J. Hydrogen Energy *42*, 13554–13567.

36. Kopp, M., Coleman, D., Stiller, C., Scheffer, K., Aichinger, J., and Scheppat, B. (2017). Energiepark Mainz: Technical and economic analysis of the worldwide largest Power-to-Gas plant with PEM electrolysis. Int. J. Hydrogen Energy *42*, 13311–13320.

37. Eichman, J., Townsend, A., and Melaina, M. (2016). Economic Assessment of Hydrogen Technologies Participating in California Electricity Markets (NREL).

38. Muradov, N. (2017). Low to near-zero CO2 production of hydrogen from fossil fuels: Status and perspectives. Int. J. Hydrogen Energy *42*, 14058–14088.

39. Parkinson, B., Balcombe, P., Speirs, J.F., Hawkes, A.D., and Hellgardt, K. (2019). Levelized cost of CO2 mitigation from hydrogen production routes. Energy Environ. Sci. *12*, 19–40.

40. Khojasteh Salkuyeh, Y., Saville, B.A., and MacLean, H.L. (2017). Techno-economic analysis and life cycle assessment of hydrogen production from natural gas using current and emerging technologies. Int. J. Hydrogen Energy *42*, 18894–18909.

41. Keipi, T., Tolvanen, H., and Konttinen, J. (2018). Economic analysis of hydrogen production by methane thermal decomposition: Comparison to competing technologies. Energy Convers. Manag. *159*, 264–273.

42. Hydrogen Council (2020). Path to hydrogen competitiveness: A cost perspective. https://hydrogencouncil.com/en/path-to-hydrogen-competitiveness-a-cost-perspective/.

43. National Renewable Energy Laboratory (2019). Annual Technology Baseline: Electricity. http://atb.nrel.gov2020/data.php.

44. Mallapragada, D.S., Pilas, D.D., Fernandez, P.G., and Martin, A.D. (2020). System implications of continued cost declines for wind and solar on driving power sector decarbonization. https://energy.mit.edu/publication/system-implications-of-continued-cost-declines-for-wind-and-solar-on-driving-power-sector-decarbonization/.

45. van Leeuwen, C., and Zauner, A. (2018). STORE&GO - Deliverable D8.3: Report on the costs involved with PtG technologies and their potentials across the EU.

46. Saba, S.M., Müller, M., Robinius, M., and Stolten, D. (2018). The investment costs of electrolysis – A comparison of cost studies from the past 30 years. Int. J. Hydrogen Energy *43*, 1209–1223.

47. Fuel Cells and Hydrogen Joint Undertaking (2014). Development of Water Electrolysis in the European Union. https://www.fch.europa.eu/node/783.

48. Ahluwalia, R.K., Papadias, D.D., Peng, J.-K., and Roh, H.S. (2019). System Level Analysis of Hydrogen Storage Options (Argonne National Laboratory).

49. Bryce, R., Losada Carreño, I., Kumler, A., Hodge, B.M., Roberts, B., and Brancucci Martinez-Anido, C. (2018). Consequences of neglecting the interannual variability of the solar resource: A case study of photovoltaic power among the Hawaiian Islands. Sol. Energy *167*, 61–75.

50. Ayers, K.E., Anderson, E.B., Capuano, C., Carter, B., Dalton, L., Hanlon, G., Manco, J., and Niedzwiecki, M. (2010). Research Advances towards Low Cost, High Efficiency PEM Electrolysis. In ECS Transactions (The Electrochemical Society), pp. 3–15.

51. IEA Greenhouse Gas R&D Programme (2017). Techno-Economic Evaluation of SMR Based Standalone (Merchant) Hydrogen Plant with CCS. https://ieaghg.org/exco_docs/2017-02.pdf.

52. U.S. Environmental Protection Agency (2018). Greenhouse Gas Reporting Program (GHGRP). https://www.epa.gov/ghgreporting/ghg-reporting-program-data-sets.

53. California Air Resources Board (2019). Monthly LCFS Credit Transfer Activity Reports. https://ww3.arb.ca.gov/fuels/lcfs/credit/lrtmonthlycreditreports.htm.

54. California Energy Commission (2018). State Electricity Generation: 2017. https://www.energy.ca.gov/data-reports/energy-almanac/california-electricity-data/2018-total-system-electric-generation/2017.

55. U.S. Energy Information Administration (2019). California Electricity Profile 2017. https://www.eia.gov/electricity/state/california/index.php.

56. Congressional Research Service (2019). Renewable Energy and Energy Efficiency Incentives: A Summary of Federal Programs. https://fas.org/sgp/crs/misc/R40913.pdf.

57. National Renewable Energy Laboratory (NREL) (2019). National Solar Radiation Database (NSRDB). https://nsrdb.nrel.gov/.

58. Sandia National Laboratories (2018). PV Performance Modeling Collaborative. https://pvpmc.sandia.gov/.

59. Bolinger, M., Seel, J., and Robson, D. (2019). Utility-scale Solar: Empirical Trends in Project Technology, Cost, Performance, and PPA Pricing in the United States – 2019 Edition (Berkeley Lab).

60. Penev, M., Rustagi, N., Hunter, C., and Eichman, J. (2019). Energy Storage: Days of Service Sensitivity Analysis (NREL).

61. Parks, G., Boyd, R., Cornish, J., and Remick, R. (2014). Hydrogen Station Compression, Storage, and Dispensing Technical Status and Costs (NREL).

62. Penev, M., and Hunter, C. (2019). Energy Storage Analysis (NREL).

Cell Reports Physical Science, Volume *1*

Supplemental Information

Can Industrial-Scale Solar Hydrogen Supplied from Commodity Technologies Be Cost Competitive by 2030?

Dharik Sanchan Mallapragada, Emre Gençer, Patrick Insinger, David William Keith, and Francis Martin O'Sullivan

Supporting information

Note S1. Model description

We evaluate the levelized cost of H_2 production for the process of Figure 1 using an integrated design and operations optimization model, described in Equations S1-S21. The model determines the capacity of individual components (e.g. PV, electrolyzer) and their hourly operating profile that minimizes the total cost of producing H_2 at the specified hourly rate, while considering various operational constraints. The objective function (Eq.S1) to be minimized includes: 1) annualized capital costs of PV, electrolysis, inverter battery energy storage, inverter, compressor and H_2 storage tanks, 2) annual fixed operating costs of PV, battery energy storage, and electrolyzer, 3) variable operating costs of battery operation and electrolyzer operation (feed water cost) 4) the cost penalty of not meeting specified hourly H_2 production targets, and 5) revenue obtained from sale of excess electricity to the grid as per the pre-specified hourly electricity prices. The results presented in this study do not consider any revenue from grid electricity exports. Similar to other studies on preliminary economics of electrolytic H_2 production [1,2], we assume that the cost of feed water as being constant across for all locations. As an example, feed water cost of \$0.002375/gal, which is the value assumed for the H2A analysis[3], translates into \$0.08/kg of H_2 produced for the assumed plant size

$$
\begin{aligned}
Minimize\ (&1000CAPEX_{PV}vPVCap + 1000CAPEXPower_{Bat}vBatPowCap \\
&+ 1000CAPEXEnergy_{Bat}vBatEnergyCap + 1000CAPEX_{Ely}vElyCap + \\
&1000CAPEX_{Inv}vInvCap + 1000CAPEX_{Comp}CompCap + \\
&CAPEX_{H2st}H2stTankCapvNumTanks) \times CCF \\
&+1000FOM_{PV}vPVCap + 1000FOM_{Bat}vBatPowCap + 1000FOM_{Ely}vElyCap \ + \\
&\sum_{t\in} VOM_{PV}vP_{PV,Tot,t} \ + \sum_{t\in T} VOM_{Ely}vP_{DCBlk,Ely.t} \\
&+ \sum_{t\in T} VOM_{Bat}(\eta_c vStCharge_t + \eta_D{}^{-1} vStDischarge_t) \ + \\
&\textstyle\sum_t \left(vFH2_{Ely,Prod,t} + vFH2_{Ely,H2st,t}\right) pFeedH2OCostEly \\
&+ SlackCost * \textstyle\sum_{t\in T} vSlack_t \ - \sum_{\{t\}} vP_{ACPow,Grid,t}\, LMP_t
\end{aligned}
\qquad \text{(S1)}
$$

We model continuous H_2 production to normally be within a band but allow the plant to shut down, defined via Eq. S2. We allow infeasible models to deviate from the required band and downtime constraints via the slack variables in Eq. S2. The high cost penalty (\$$10^6$/kg) on the slack variables ensures that the model prioritizes feasibility over reducing costs by violating production commitments. The power output from the PV unit at each hour is either directly utilized or used to charge battery storage for later use (Eq. S3). The hourly output of the PV arrays is limited by their resource availability as per Eq. S4. Inter-temporal constraints given by Eq. S5-S9 characterize the operation of the battery, where Eq. S5 governs that the charge at the end of time period *t* is equal to the sum of the charge at the end of the previous time period (*t-1*) and the net charging, after accounting for any discharging, occurring during period *t*. Further, the state of charge in the first period of the year (t=1) is endogenously determined by relating it to the state of charge for the last period of the year (t=8760) via Eq. S6. This "wrapping" constraint is often used to initialize the state of charge of energy storage devices when modeling a single

year of operations [4]. Eq. S7-S8 limit the rate of charge and discharge of battery storage to be less than the installed battery power rating at all times, while Eq. S9 ensures that the total stored energy does not exceed the installed capacity at all times. Eq. S10 constrains the maximum energy capacity of the battery such that it can be provide *pDurUB* hours of power at the rated power capacity, *vBatPowerCap*.

As per Eq. S11, the DC power supplied from the PV array and battery storage at each hour is balanced against the power demand from the electrolyzer and the compressor (via the inverter). It is worth noting that the DC coupling of PV and electrolyzer systems assumed here, is not yet commercially proven. H_2 production from the electrolyzer is modeled using a constant specific power consumption and the produced H_2 is distributed to between end use and storage to meet production requirements at a later time (Eq. S12). We don't explicitly model the cost or energy requirements for purification of feed water or produced H_2 (e.g. drying), but rather assume the cost and specific energy consumption of the electrolysis system are inclusive of these conditioning units. Eq. S13 stipulates that the power input to the electrolyzer cannot exceed the installed capacity at all times.

Eq. S14 enforces that the AC power output from the inverter is either consumed for operating the H_2 compressor or exported to the grid. The inverter and compressor capacities are sized to meet the maximum power flows through each device (Eq. S15-S16). Eq. S17 calculates the compressor power requirement for each time period as a function of the H_2 flow rate sent to storage. We assume constant specific compression power for compressing H_2 from the electrolyzer pressure (20-30 bar as per state-of-art PEM electrolyzers [5]) to the design pressure for H_2 storage (~100 bar) , although in practice, the dynamics of storage charging/discharging may result in time-varying specific compression power. The effect of this approximation on model results is partly mitigated by two factors: 1) the compression energy requirements are approximately an order magnitude smaller than the electrolyzer energy requirements and 2) the prospect of excess electricity from PV during times of compressor operation, especially in the summer season, since the PV array is sized larger than the electrolyzer (Figure 2). The constraints defining the state of charge of H_2 storage (Eq. S18-S20) are similar to the constraints used to model battery energy storage, with the only distinction being that we do not account for any energy losses during charging and discharging. The parasitic losses associated with H_2 compression, however, are accounted via Eq. S17. Note that this analysis assumes that the H_2 storage can fully discharged, even though operating protocols for pressurized gas storage may mandate a minimum H_2 storage level to maintain a minimum pressure level in the storage [3]. E q. S20 constraints the maximum amount of $_{H2}$ stored at any time period to be limited by the installed capacity of H2 storage.

The requirement on annual plant availability is enforced via Eq. S21, which states that the number of hours when the plant is online should be atleast equal to the stipulated availability requirements. Further, we enforce via Eq. S22-S24, that plant downtime periods must be atleast of duration defined by the parameter, *MinOffline*, to mimic typical outage schedules for existing H_2 production facilities for maintenance etc.

$$vProd_t * DesignFH2 * UtilizationFactor - vSlack_t \leq vFH2_{H2st,Prod,t} + vFH2_{Ely,Prod,t} \leq vProd_t * DesignFH2 + vSlack_t \; \forall t \quad (S2)$$

$$vStCharge_t + vP_{PV,DCBlk,t} = vP_{PV,Tot,t} \quad \forall t \quad (S3)$$

$$vP_{PV,Tot,t} \leq CF_t \times vPVCap \; \forall t \quad (S4)$$

$$vStSoC_{t,st} = vSoC_{t-1,st} + \eta_{c,st} vStCharge_{t,st} - \eta_D{}^{-1} vStDischarge_t \; \forall t \in [2, 8760] \quad (S5)$$

$$vStSoC_t = vStSoC_{8760} + \eta_c vStCharge_t - \eta_D{}^{-1} vStDischarge_t \; \forall \; t = 1 \quad (S6)$$

$$\eta_c vStCharge_t \leq vBatPowCap \;\; \forall \; t \quad (S7)$$

$$\eta_D{}^{-1} vStDischarge_t \leq vBatPowCap \; \forall \; t \quad (S8)$$

$$vStSOC_t \leq vBatEnergyCap \; \forall \; t \quad (S9)$$

$$vStSOC_t \leq DurUB \times vBatPowCap \;\; \forall \; t \quad (S10)$$

$$vP_{PV,DCBlk,t} + vStDischarge_t = vP_{DCBlk,Ely,t} + vP_{DCBlk,Inv,t} \; \forall t \quad (S11)$$

$$\frac{1000 vP_{DCBlk,Ely,t}}{SpecPower_{Ely}} = vFH2_{Ely,Prod,t} + vFH2_{Ely,H2st,t} \; \forall t \quad (S12)$$

$$vP_{DCBlk,Ely,t} \leq vElyCap \;\; \forall t \quad (S13)$$

$$\eta_{inv} vP_{DCBlk,Inv,t} = vP_{ACPow,Comp,t} + vP_{ACPow,Grid,t} \; \forall t \quad (S14)$$

$$vP_{DCBlk,Inv,t} \leq vInvCap \;\; \forall t \quad (S15)$$

$$vP_{ACPow,Comp,t} \leq vCompCap \;\; \forall t \quad (S16)$$

$$\frac{SpecPower_{Comp} vFH2_{Ely,H2St,t}}{1000} = vACPowToComp_t \; \forall t \quad (S17)$$

$$vH2stSoC_t = vH2stSoC_{8760} + vFH2_{Ely,H2st,t} - vFH2_{H2st,Prod,t} \;\; , t = 1 \quad (S18)$$

$$vH2stSoC_t = vH2stSoC_{t-1} + vFH2_{Ely,H2st,t} - vFH2_{H2st,Prod,t} \; \forall t \in [2,8760] \quad (S19)$$

$$vH2stSoC_t \leq vH2stTankCap \; \forall t \quad (S20)$$

$$\sum_{t \in T} vProd_t \geq 8760 AvailReq \quad (S21)$$

$$vProd_{t-i} - vProd_{t-i-1} \leq 1 - vProd_t \; \forall \; t \in T \; \forall \; i \in \{1, \dots, MinOffline\} \mid t - i > 1 \quad (S22)$$

$$vProd_1 - vProd_{8760} \leq 1 - vProd_t \; \forall \; t \in T \; \forall \; i \in \{1, \dots, MinOffline\} \mid t - i = 1 \quad (S23)$$

$$vProd_{8760+t-i} - vProd_{8760+t-i-1} \leq 1 - vProd_t \; \forall \; t \in T \; \forall \; i \in \{1, \dots, MinOffline\} \mid \; t - i < 1 \quad (S24)$$

Table S 1. Indices and sets

Symbol	Description
$st \in ES$	Set of battery energy storage technologies
$t \in T$	Time periods of facility operation (default: 8760 hours per year)

Table S 2. Model parameters

Symbol	Units	Description
$CAPEX_{PV}$	$/kW	Capital cost of PV (DC)
$CAPEXPower_{Bat}$	$/kW	Power capital cost of battery energy storage technology
$CAPEXEnergy_{Bat}$	$/kW	Energy capital cost of battery energy storage technology
$CAPEX_{Ely}$	$/kW	Capital cost of electrolyzer (PEM)

$CAPEX_{Inv}$	$/kW	Capital cost of DC to AC inverter
$CAPEX_{Comp}$	$/kW	Capital cost of H_2 compressor
$CAPEX_{H2st}$	$/kg	Capital cost of H_2 storage tanks
FOM_{PV}	$/kW/yr	Fixed operating cost of PV system
FOM_{Bat}	$/kW/yr	Fixed operating cost of battery storage system of type *st*
FOM_{Ely}	$/kW/yr	Fixed operating cost of electrolyzer (PEM)
VOM_{PV}	$/MWh	Variable operating cost of PV system
VOM_{Ely}	$/MWh	Variable operating cost of electrolyzer (PEM)
$VOM_{Bat,st}$	$/MWh	Variable operating cost of battery storage of type *st*
VOM_{comp}	$/MWh	Variable operating cost of compressor
VOM_{H2st}	$-hr/kg	Variable operating cost of compressor
CF_t	%	Hourly PV availability as a percentage of its peak capacity
η_C	%	Charging efficiency of battery energy storage of type *st*
η_D	%	Discharging efficiency of battery energy storage of type *st*
$pDurUB$	Hours	Maximum duration of battery storage
$SpecPower_{Ely}$	kWh/kg	Electrical energy consumption of electrolyzer (PEM)
$SpecPower_{Comp}$	kWh/kg	Electrical energy consumption to compress H_2 from electrolyzer pressure (20-30 bar) to storage pressure (350-400 bar)
η_{inv}	%	Inverter efficiency
$DesignFH2$	kg/hr	Design H_2 production capacity
$UtilizationFactor$	%	Minimum hourly utilization factor for the entire facility
CCF	%	Capital charge factor, defined as the ratio of the levelized cost of capital to the overnight capital cost
$AvailReq$	%	Fraction of the time that the plant must be online
$MinOffline$	hours	Number of time periods the facility must be down if it goes offline
LMP_t	$/MWh	Wholesale electricity price at time t
$SlackCost$	$/kg	Cost penalty for not meeting hourly H_2 production targets (default =10^6)

Table S 3. Model decision variables

Symbol	Units	Description
$vPVCap$	MW	Installed PV capacity (DC)
$vBatPowCap$	MW	Installed power capacity of battery energy storage
$vBatEnergyCap$	MWh	Installed energy capacity of battery energy storage
$vElyCap$	MW	Installed electrolyzer capacity
$vInvCap$	MW	Installed inverter capacity
$vCompCap$	MW	Installed capacity of H_2 compressor
$vStCharge_t$	MW	Power to charge battery energy storage during time t
$vStDischarge_t$	MW	Discharged power from battery energy storage during time t
$StSoC_{t,st}$	MWh	State of charge of battery energy storage during time t
$vP_{PV,Tot,t}$	MW	Power output from PV during time t
$vP_{PV,DCBlk,t}$	MW	PV power output to DC power block during time t
$vP_{DCBlk,Ely,t}$	MW	Power flow from DC power block to electrolyzer during time t
$vP_{DCBlk,Inv,t}$	MW	Power flow from DC power block to inverter during time t
$vP_{ACPow,Comp,t}$	MW	AC power consumption by H_2 compressor during time t
$vP_{ACPow,Grid,t}$	MW	AC power exported to grid during time t
$vFH2_{Ely,Prod,t}$	kg/hr	Product flow rate of H_2 sourced from electrolyzer during time t
$vFH2_{Ely,H2st,t}$	kg/hr	H_2 flow rate from electrolyzer to storage during time t
$vH2stSoC_t$	kg	State of charge of H_2 storage during time t
$vSlack_t$	kg/hr	Absolute deviation from production boundaries during time t
$vH2Tankcap$	kg	Installed capacity of H_2 storage
$vProd_t$	#	Binary variable determining plant status; 0 if plant is down during period t

Note S2. Model data inputs

Hourly PV resource availability across the U.S. is characterized as per typical meteorological year (TMY) insolation data from the NREL solar radiation database (NSRDB) [6] in conjunction with the *pvlib* toolbox simulation [7] for a single-axis PV array that is oriented horizontally. The TMY data is preferred over historical insolation data from a particular year to avoid biasing results from transitory weather effects in a given year. Table S 4 summarizes the additional cost and performance assumptions for the various components for the 2020 and 2030 scenario. All dollar values are presented in 2016 U.S. dollars, unless noted otherwise.

There is considerable variation in reported costs of electrolyzer systems, partly due to differences in assumed system size [8–10]. Our estimates for current capital costs rely on vendor information for costs for multi-MW systems. For example, [11] cites data from two vendor on stack costs, to estimate system costs of $800/kW in 2014 dollars. Other more recent publications also support our capital cost estimate for 2020 [10,12,13].

The annualized electrolyzer stack replacement costs are estimated by calculating the present value of periodical stack replacement through the project lifetime (i.e. stack replaced in year 5, 10, 15 for system lifetime of 20 years and cell lifetime of 5 years) and assuming stack cost are 50% of total system capital costs.

Table S 4. Additional technology cost and performance assumptions across 2020 and 2030 scenarios. FOM= Fixed Operation and Maintenance, VOM= Variable Operation and Maintenance. Dollar values, unless otherwise stated in 2016 dollars.

Parameters	2020	2030	Data source/comments
Capital costs			
Inverter ($/kW)	60	60	Table 4 of [14]
Capital charge factor (CCF)	10.3	10.3%	Ratio of annualized capital cost to total capital cost. Default value based on cost of capital of 8.1% and project lifetime of 20 years.
FOM costs			
Battery storage ($/kW/yr)	7.8	5.3	[15]
VOM costs			
PV ($/MWh)	0	0	[15]
Feed water costs ($/kg)	$0.015	$0.015	[15]
Storage charge/discharge ($/MWh)	3	3	Assumption
Performance parameters			
Minimum plant downtime (hours)	12		
H_2 storage tank capacity (kg)	1000		
Inverter efficiency (%)	96		Assumption

Table S 5. Brief literature review of estimated capital cost for bulk H_2 storage either in pressure vessel or geological formations.

Reference	Type	Description	Pressure range (bar)	Estimated capacity (tonnes)	Working capacity (%)	Estimated capital cost ($/kg)
[16]	Pressure vessel	Storage tanks (generic)	NA	NA	NA	1000
[17]	Pressure Vessel	Spherical vessels	1.20	0.3	100	1126
		Spherical vessels	2	0.5	100	874
		Spherical vessels	2	1.5	100	726
		Spherical vessels	2	4.6	100	548
	Spherical vessels	Pipe storage (buried underground)	100	64,714	100	346
[18]	Pressure vessel	Pipe storage	~100	50	100	516
	Geological	Salt cavern	70-190	6000	62	33
		Underground Lined Rock Cavern	150	672	95	60
[19]	Pressure vessel	Cylindrical tanks	200	10-100	-	283-503
	Geological	Salt cavern	200		-	8.8
[20]	Geological	Salt cavern	~100	2486	77	18.7
		Depleted Oil & gas reservoir	~100	2868	67	11.4
		Hard rock	~100	2486	77	32.5
		Aquifer	~100	2868	67	11.8
[21]	Geological	Salt cavern	~100	2520	-	0.8-1.6
[22]	Geological	Salt dome	-	-	-	2.69

Table S 6. Summary of average PV capacity factor and H_2 production related GHG emissions in 2017 for the evaluated sites in Figure 5 - Figure 9. PV availability is characterized using Typical Meteorological Year insolation data available from the National Solar Radiation Database [6]. H_2 related GHG emissions from existing H_2 production facilities as per the 2017 edition of the GHG reporting program [23]. The selected sites represent the top 10 sites in terms of PV capacity factor with existing H_2 production.

Location label	Average annual PV capacity factor	H_2 related GHG emissions in 2017 (Million tonnes CO_2eq per year)	Share of total H_2-related GHG emissions (%)	State	Latitude	Longitude
L1	0.22	0.53	1.19	TX	27.93	-97.34

L2	0.22	4.1	9.31	CA	38.09	-121.82
L3	0.23	4.3	9.74	CA	34.13	-117.9
L4	0.23	0.05	0.10	CA	38.65	-121.82
L5	0.24	0.03	0.07	CA	35.25	-118.9
L6	0.24	0.51	1.14	TX	35.81	-101.26
L7	0.24	0.23	0.51	TX	35.81	-102.22
L8	0.24	1.19	2.67	CA	34.13	-118.9
L9	0.26	0.15	0.34	NM	33.01	-104.18
L10	0.27	0.03	0.06	TX	31.85	-106.1

Note S3. Solution methodology

The integrated operations and design optimization model was implemented in Pyomo [24] and solved using a commercial mixed-integer linear programming (MILP) model solver, Gurobi [25] on a high performance computing cluster available at MIT.

The results on levelized H_2 productions for the continental U.S., are based on outputs of the integrated design and operations optimizations model for 1487 terrestrial locations. These results assign zero value to the excess electricity available from the sized PV system that is not utilized for H_2 production. The 1487 locations studied were identified as grid points of a 2-dimensional grid consisting of 60 uniformly spaced latitudes and 45 uniformly spaced latitude covering the entire continental U.S. land area. For each location, we solved the optimization model described in S.1. while fixing the variable corresponding to grid exports ($vP_{ACPow,Grid,t}$) to be zero. Subsequently, we generated the spatial maps for levelized H_2 production costs, shown in Figure 4, by generating a Voronoi diagram over the evaluated grid points. The Voronoi diagram creates a visualization in which the color of each point is representative of the levelized H_2 cost of the nearest point evaluated via the optimization model. For high density grids, this is a good approximation and is easier to read than a scatter plot.

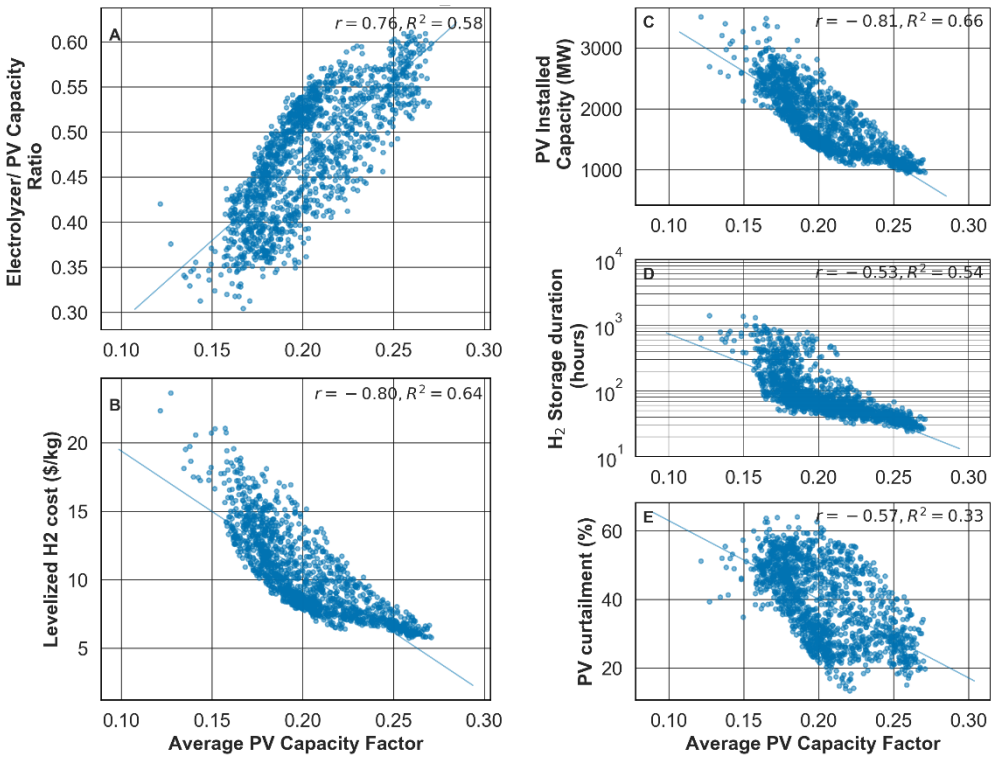

Figure S 1.Cost-optimal design trends for continuous H_2 production of 100 tonnes/ day (4.17 tonnes/hour) with 95% availability for various locations in the U.S., characterized by annual average PV capacity factor. Results based on co-optimizing facility design and operation over the entire year at an hourly resolution for the 2020 cost scenario with pressure vesse H_2l storage defined in Table 1 and Table S 4. Each point represents the design outcome for a different location in the U.S. and the line corresponds to the least-square linear fit of the data. ***a)*** *Ratio of installed electrolyzer capacity to PV capacity,* ***b)*** *levelized H_2 production cost,* ***c)*** *PV installed capacity (MW),* ***d)*** *H_2 storage duration,* ***e)*** *PV curtailment as a percent of available generation. r: correlation coefficient; R^2: coefficient of determination of the linear fit shown for each figure. In all cases, the model deploys zero battery storage capacity and hence the trends in battery storage size are not shown. PV availability characterized using Typical Meteorological Year insolation data available from the National Solar Radiation Database [6]. Duration of H_2 storage calculated by dividing the capacity of installed H_2 storage (in tonnes) with the design flow rate (4.17 tonnes/hour).*

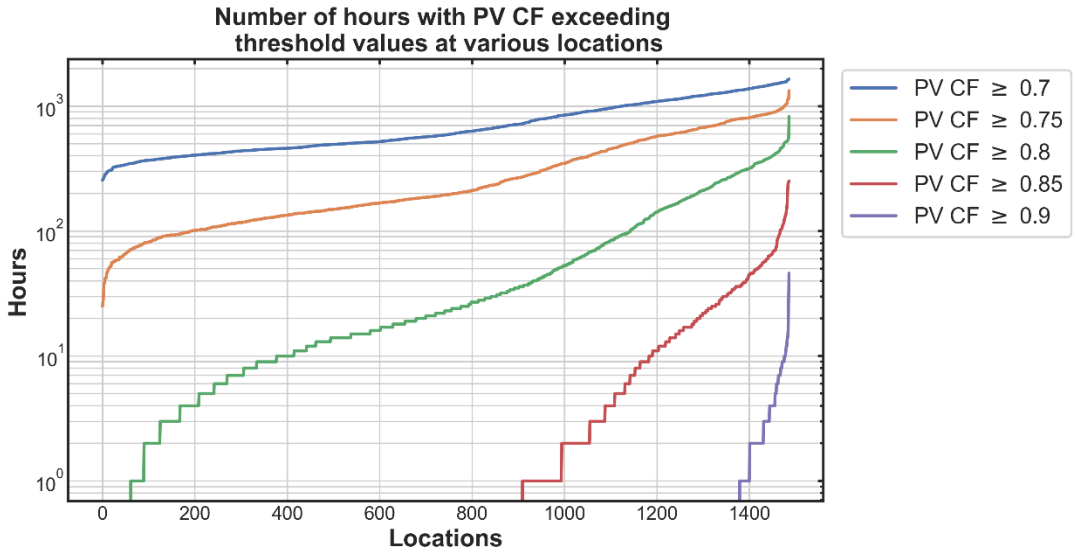

Figure S 2. Distribution in the number of hours with high PV capacity factor (CF) across 1487 U.S. locations evaluated in this study. PV availability characterized using Typical Meteorological Year insolation data available from the National Solar Radiation Database [6]

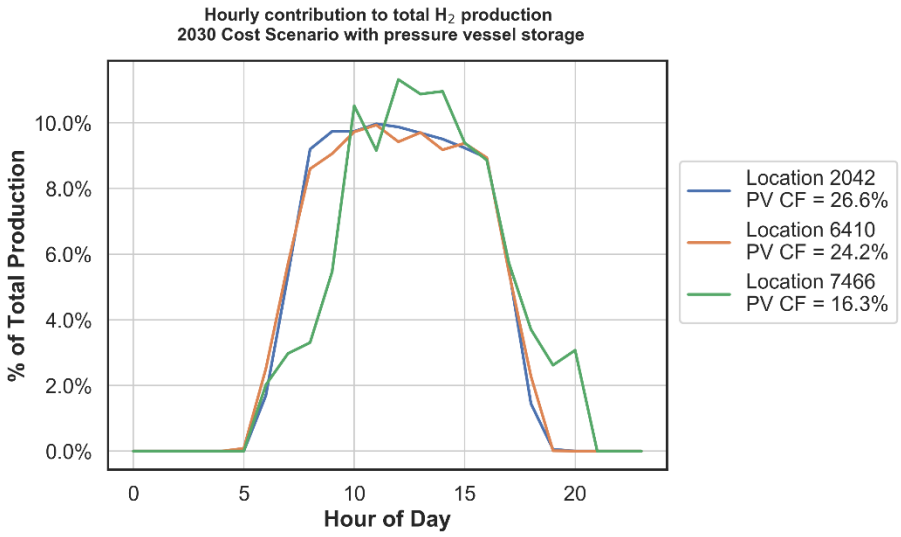

Figure S 3. Share of total annual H_2 produced at different hours of the day across three different locations with differing PV resource quality. Results based on outputs of integrated design and optimization model (see S.1) using 2030 cost scenario with pressure vessel H_2 storage, defined in Table 1 and Table S 4. PV resource in each location characterized using insolation data for Typical Meteorological Year (TMY) available from the National Solar Radiation Database [6]*. PV CF = PV capacity factor, annual average value.*

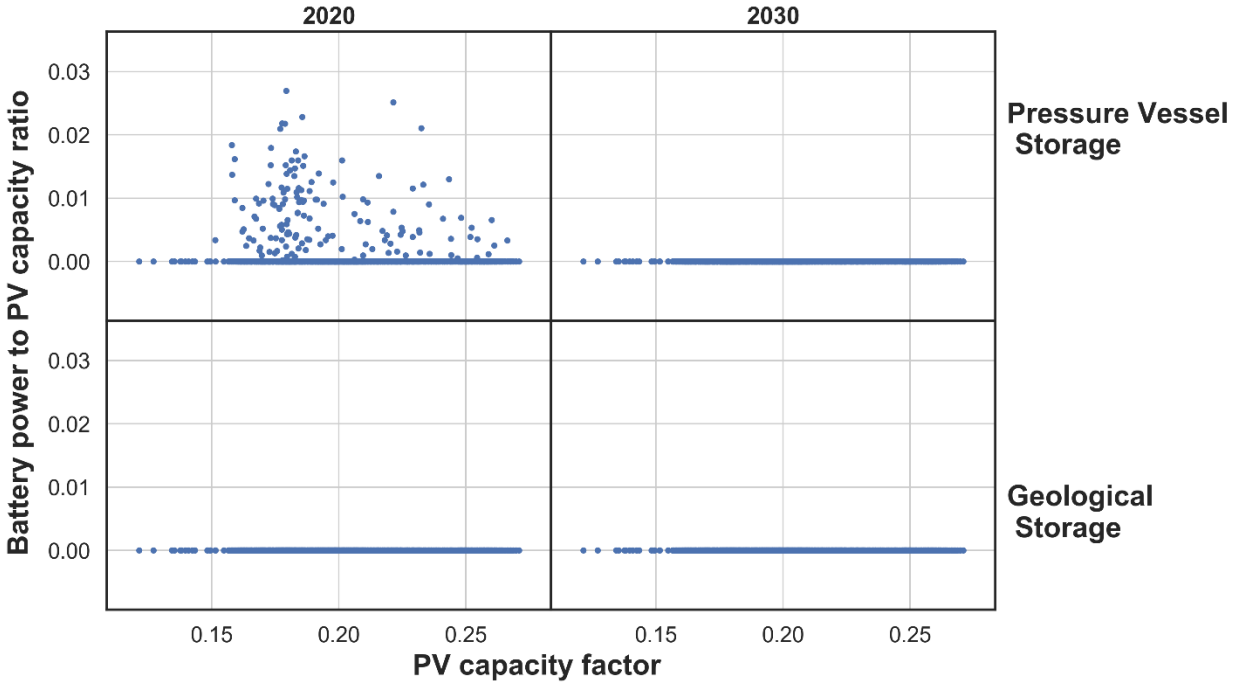

Figure S 4. Installed battery storage power capacity (reported relative to PV capacity) for the cost-optimal design of a PV-electrolytic H_2 production facility, as a function of location, characterized by annual average PV capacity factor (x-axis), cost scenario (2020, 2030) and storage type (pressure vessel or geological). Results based on modeling continuous H_2 production of 100 tonnes/day (4.17 tonnes/hour, with 10% hourly tolerance) with 95% annual availability at each location. Each point represents the design outcome for a different location in the U.S.

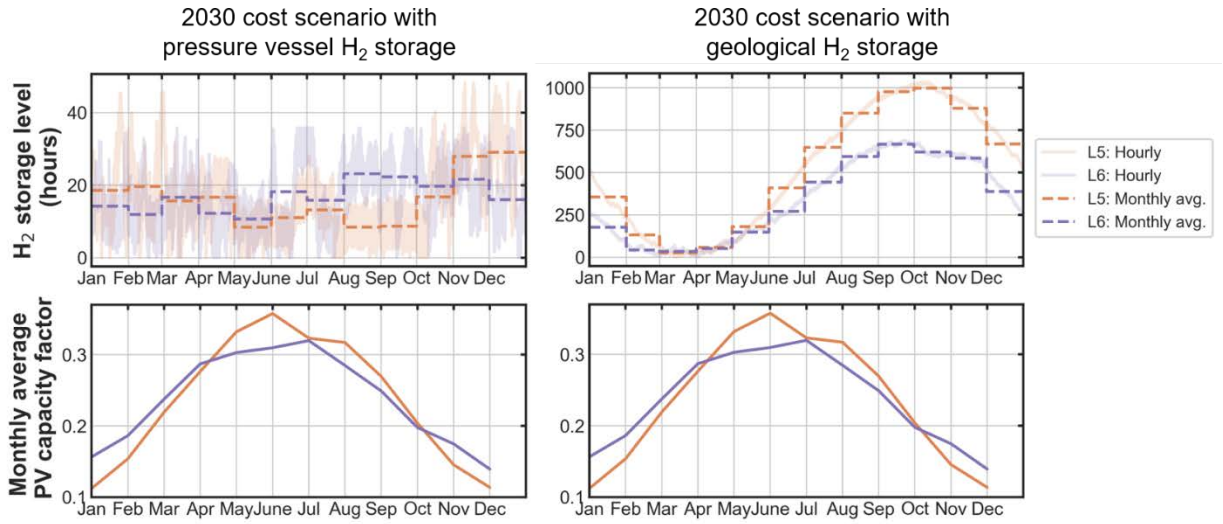

Figure S 5. Annual variations in H_2 storage levels (top) and PV availability (bottom) for two hypothetical PV-electrolysis facilities with similar average PV capacity factor, producing 4.17 tonnes /hour H_2 (100 tonnes/day, with 10% hourly tolerance and 95% annual availability). The labels "L5" and "L6" refer to the location with same labels defined in Figure 5 and correspond to sites with annual average capacity factor of 23.6% and 23.7%, respectively. Left and right charts on the top row correspond to model results with pressure vessel H_2 storage and geological H_2 storage, respectively. Dotted lines in the top row refer to monthly average storage inventory levels for the two sites. The time units used for displaying H_2 storage are estimated by dividing the hourly inventory of stored

H_2 (in kg) with the nominal design flow rate of 4.17 tonnes H_2 per hour. Results shown correspond to the 2030 scenario defined in Table 1.

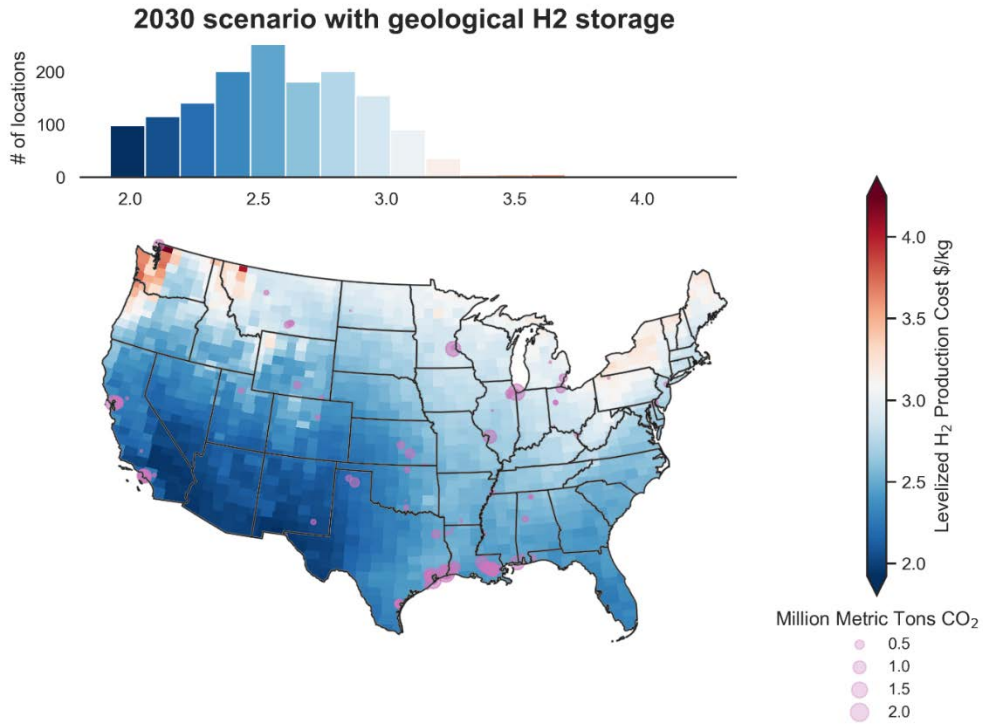

Figure S 6. Spatial distribution in levelized costs of round-the-clock H_2 production for an integrated PV-electrolysis-storage facility for the 2030 scenario with geological H_2 storage, defined in Table 1 and Table S 4. The visualization is based on defining Voronoi polygons (see SI (section S.3.1)) from cost estimated at 1487 grid points using the integrated design and optimization model. PV resource in each location characterized by typical meteorological year insolation data available from the NREL solar radiation database [48]. Pink markers indicate location of existing H_2 production facilities as per the 2017 edition of the EPA GHG reporting program [49], with size of the marker proportional to annual GHG emissions attributed H_2 production at the facility in 2017.

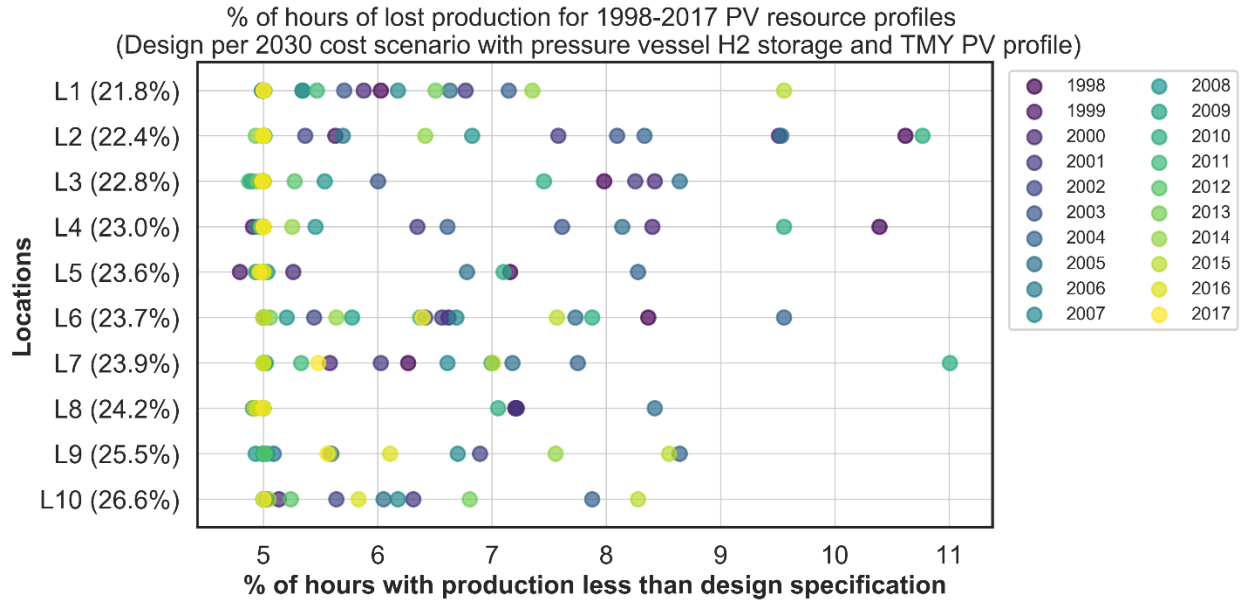

Figure S 7. Impact of inter-annual variations in PV availability (1998-2017) on the number of hours with production less than minimum design specification (90% of 4.17 tonnes/hour) for a H_2 production facility sized using Typical Meteorological Year (TMY) data. Results are shown for 10 locations, identified in Figure 5, for the 2030 cost scenario with for pressure vessel H_2 storage, as defined in Table 1

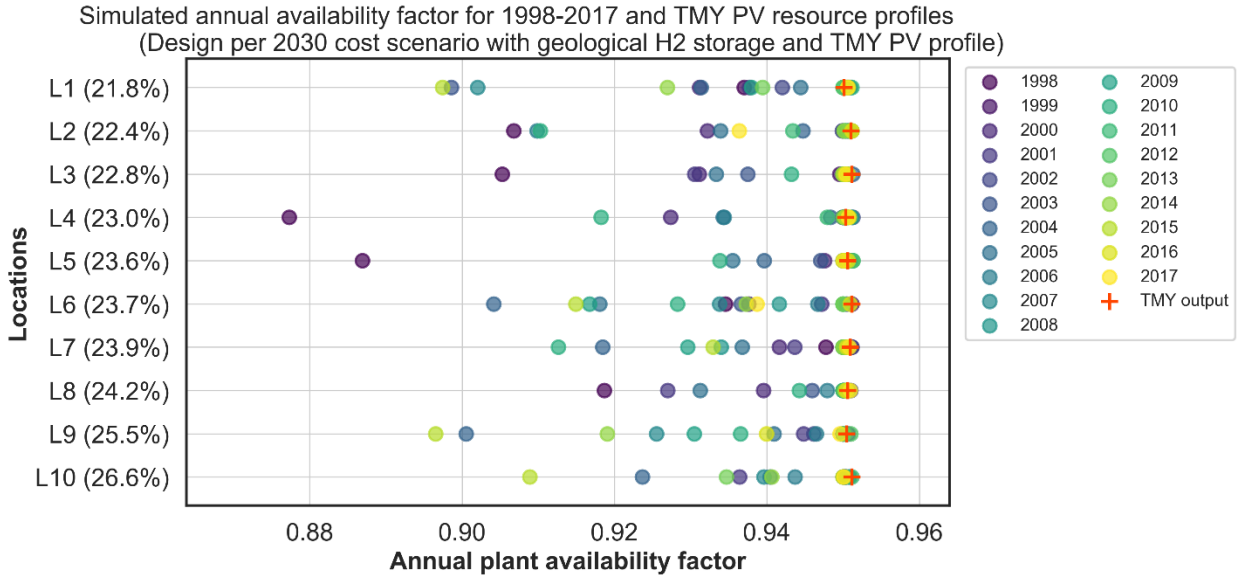

Figure S 8. Simulated annual plant availability factor for a H_2 production facility sized using solar resource characterized using Typical Meteorological Year (TMY) data using historical PV resource availability profiles for 1998-2017 (colored circles). Plant availability factor is defined as the ratio of total annual H_2 production of the facility for each weather year (historical or TMY) relative to the design amount (after derating for maximum deviation in hourly flow rate of 10%). Results are shown for 10 locations, identified in Figure 5, for the 2030 cost scenario with for geological H_2 storage, as defined in Table 1

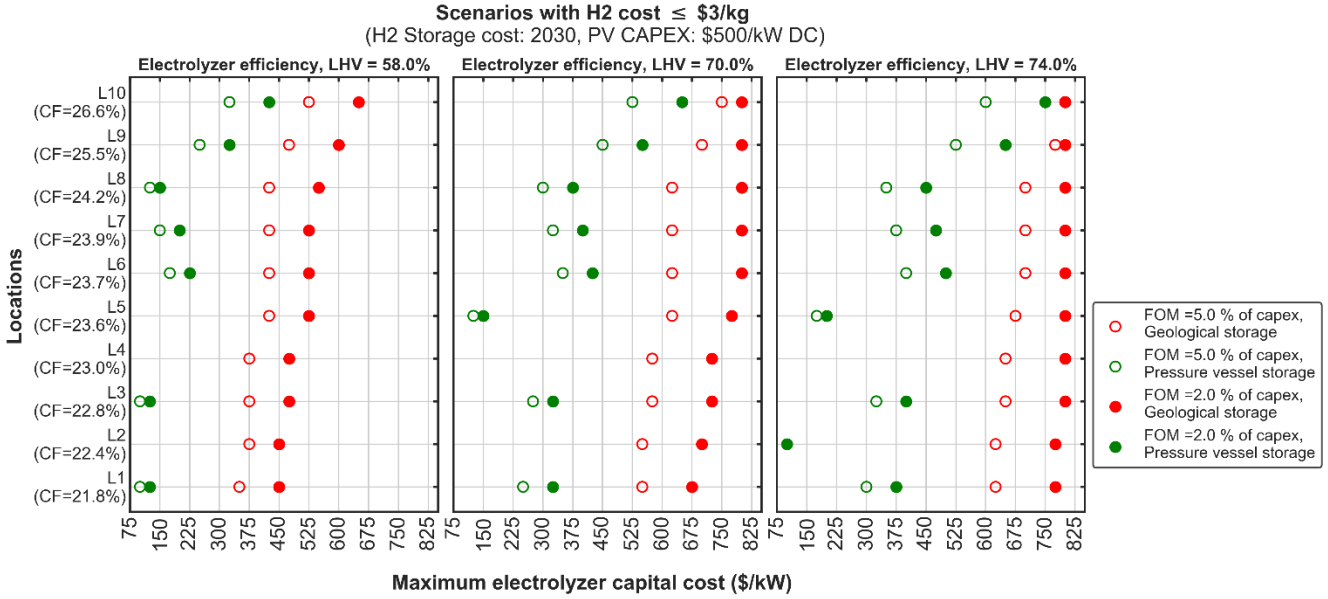

Figure S 9. Combination of parameter values for electrolyzer capital costs, fixed operating and maintenance (FOM) costs, energy efficiency (based on lower heating value (LHV)) and H_2 storage capital costs that result in levelized

costs less than or equal to $3/kg. Cost of geological and pressure vessel H_2 storage are equal to $3/kg and $345/kg, respectively, corresponding to the 2030 cost scenario. Cost of remaining parameters are defined under the "2030" column in Table 1 and Table S 4. For each location, points are marked for only those combination of parameter values which results in costs lower than $3/kg. Filled and empty circles correspond to FOM costs equal to 2% and 5% of capital costs, respectively. The circle colors are used to designate whether system uses pressure vessel or geological H_2 storage.

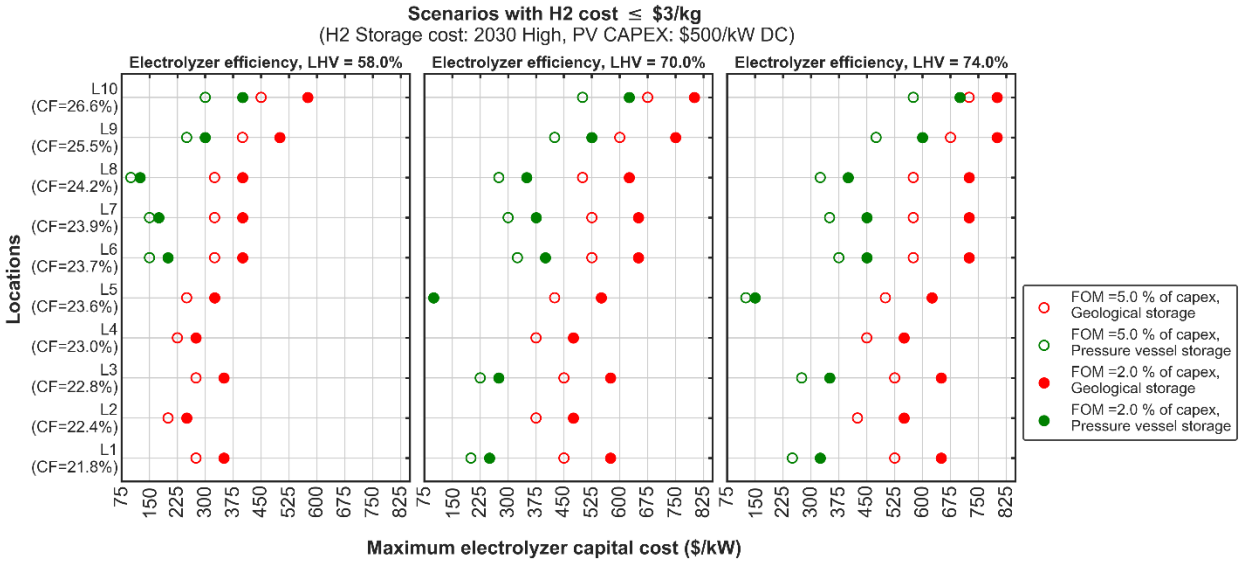

Figure S 10. Combination of parameter values for electrolyzer capital costs, fixed operating and maintenance (FOM) costs, energy efficiency (based on lower heating value (LHV)) and H_2 storage capital costs that result in levelized costs less than or equal to $3/kg. Cost of geological and pressure vessel H_2 storage are equal to $33/kg and $516/kg, respectively, corresponding to the 2020 cost scenario. Cost of remaining parameters are defined under the "2030" column in Table 1 and Table S 4. For each location, points are marked for only those combination of parameter values which results in costs lower than $3/kg. Filled and empty circles correspond to FOM costs equal to 2% and 5% of capital costs, respectively. The circle colors are used to designate whether system uses pressure vessel or geological H_2 storage.

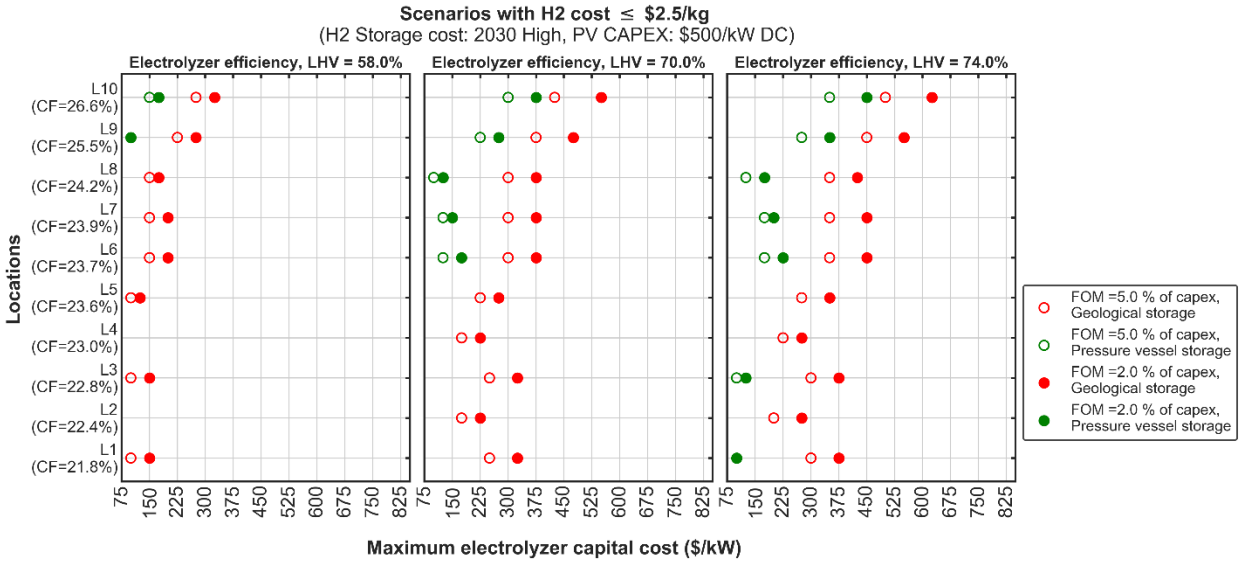

Figure S 11. Combination of parameter values for electrolyzer capital costs, fixed operating and maintenance (FOM) costs, energy efficiency (based on lower heating value (LHV)) and H_2 storage capital costs that result in levelized

costs less than or equal to \$2.5/kg. Cost of geological and pressure vessel H_2 storage are equal to \$33/kg and \$516/kg, respectively, corresponding to the 2020 cost scenario. Cost of remaining parameters are defined under the "2030" column in Table 1 and Table S 4. For each location, points are marked for only those combination of parameter values which results in costs lower than \$2.5/kg. Filled and empty circles correspond to FOM costs equal to 2% and 5% of capital costs, respectively. The circle colors are used to designate whether system uses pressure vessel or geological H_2 storage.

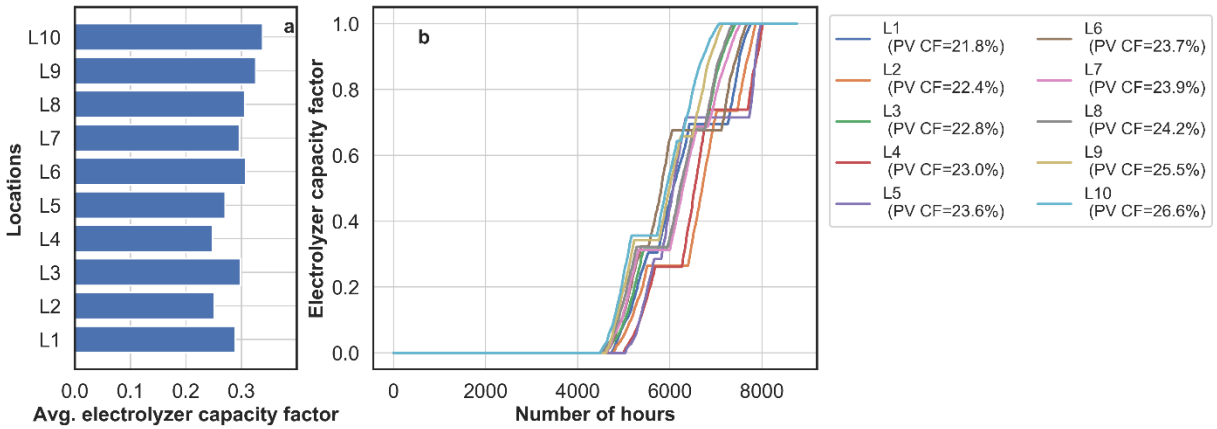

*Figure S 12. Trends in electrolyzer capacity utilization for producing 4.17 tonnes H_2 per hour (within 10% tolerance) with 95% availability at various locations under the 2030 scenario using pressure vessel H2 storage (see Table S 4). **a)** annual average electrolyzer capacity factor and **b)** distribution of hourly capacity factor for electrolyzer. Location labels, L1 to L10, refer to the locations denoted in the map of Figure 5.*

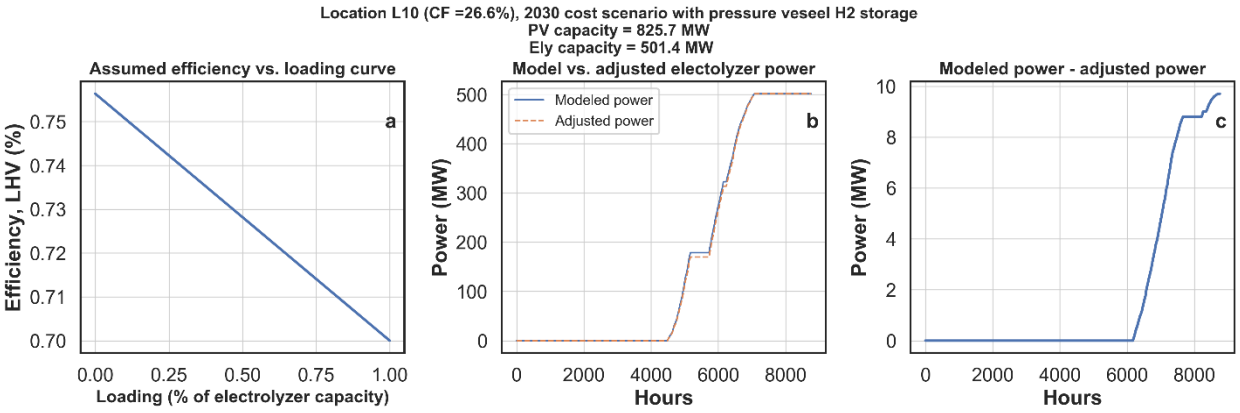

*Figure S 13. Impact of varying electrolyzer energy efficiency with loading on electrolyzer hourly power consumption at a single location for the 2030 cost scenario with pressure vessel H_2 storage (see Table S 4). Results based on process design criteria of producing 4.17 tonnes /hour (within 10% tolerance) with 95% availability. **a)** Assumed variation in efficiency as a function of loading, **b)** Distribution of hourly power consumption under the constant efficiency case and the case with efficiency variation with loading level, **c)** difference between modeled power with constant efficiency assumption and power consumption based on efficiency variation with loading as per panel a. Location labels L10, correspond to the location with the same name defined Figure 5.*

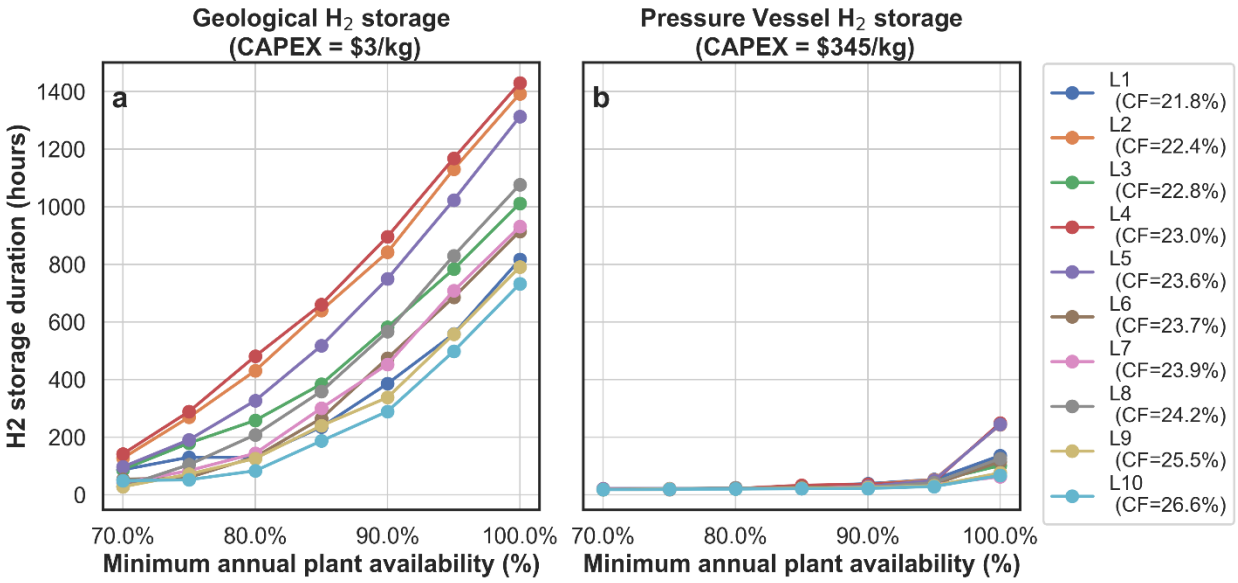

Figure S 14. Impact of changes in minimum plant availability requirements on the duration of installed H_2 storage capacity for different H_2 storage capital costs and at various locations in the U.S. Location labels, L1 to L10, refer to the locations with the same name defined in Figure 5. Aside from storage capital costs, cost of other input parameters correspond to the 2030 scenario defined in Table 1 and Table S 4. Hourly H_2 production requirement held constant across the differing plant availability requirement cases at 4.17 tonnes per hour (with 10% hourly tolerance). Duration of H_2 storage calculated by dividing the capacity of installed H_2 storage (in kg) with the design flow rate (4.17 tonnes /hour).

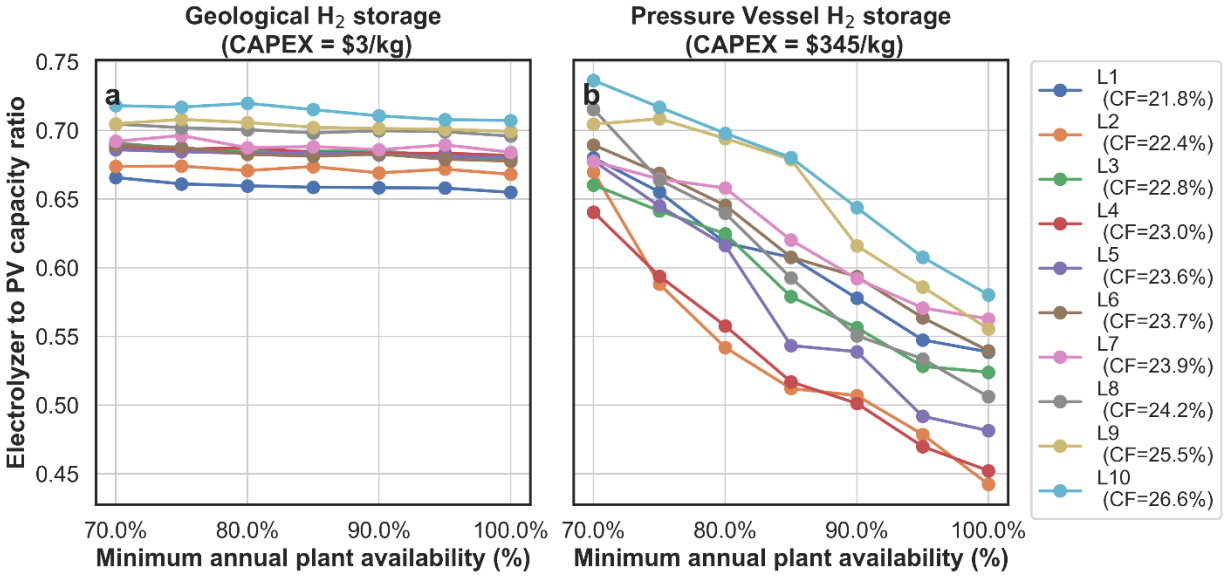

Figure S 15. Impact of changes in minimum plant availability requirements on the ratio of electrolyzer to PV capacity for different H_2 storage capital costs and at various locations in the U.S.. Location labels, L1 to L10, refer to the locations with the same name defined in Figure 5. Aside from storage capital costs, cost of other input parameters correspond to the 2030 scenario defined in Table 1 and Table S 4. Hourly H_2 production requirement held constant across the differing plant availability requirement cases at 4.17 tonnes per hour (with 10% hourly tolerance).

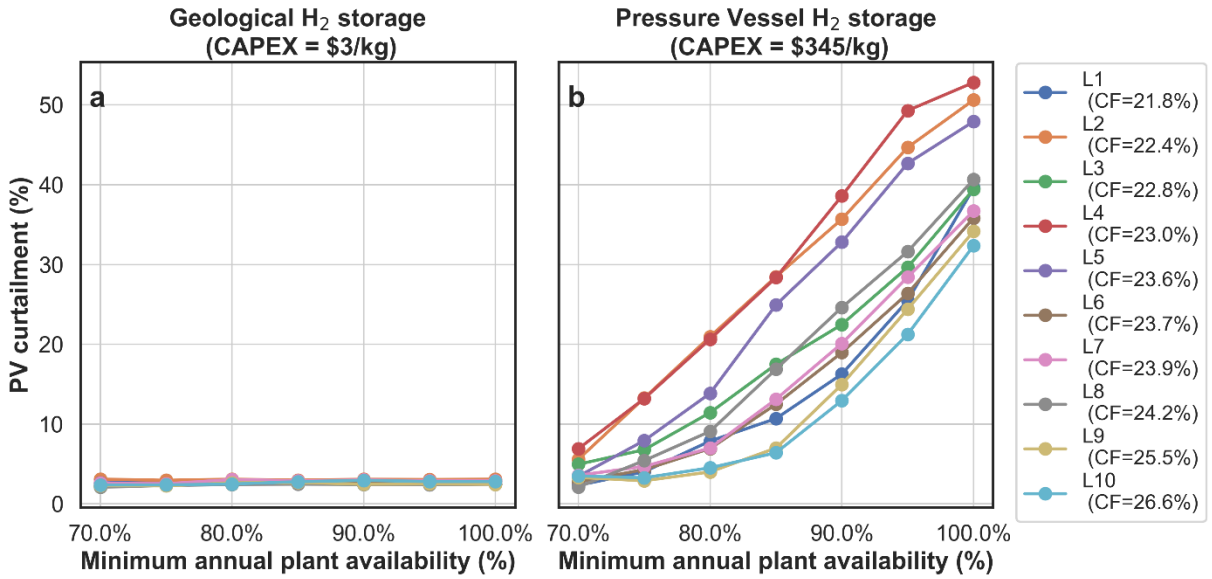

Figure S 16. Impact of changes in minimum plant availability requirements on annual PV curtailment for different H_2 storage capital costs and at various locations in the U.S. Location labels, L1 to L10, refer to the locations with the same name defined in Figure 5. Aside from storage capital costs, cost of other input parameters correspond to the 2030 scenario defined in Table 1 and Table S 4. Hourly H_2 production requirement held constant across the differing plant availability requirement cases at 4.17 tonnes per hour (with 10% hourly tolerance).

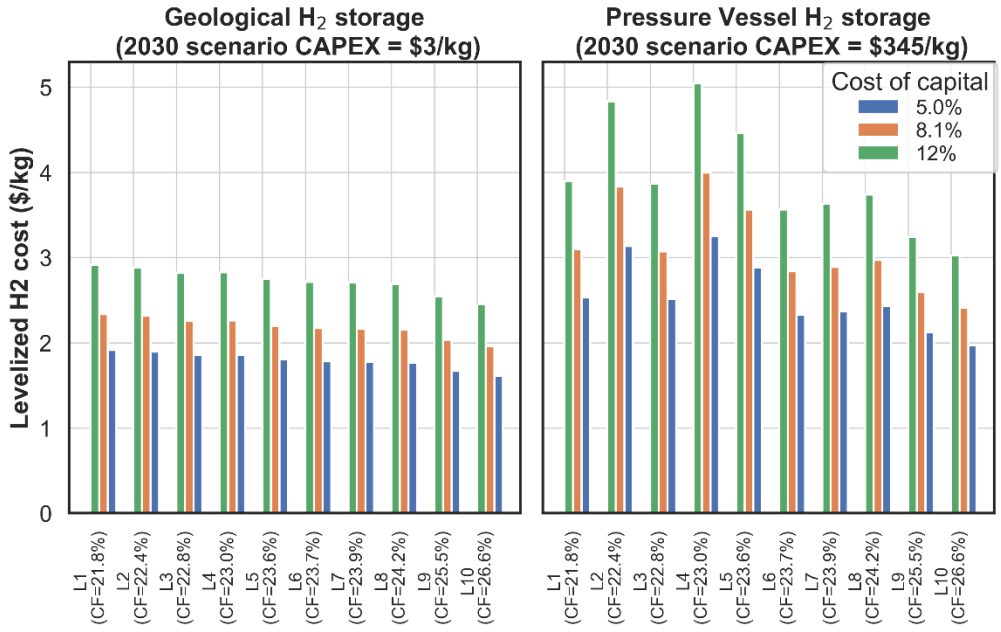

Figure S 17. Sensitivity of levelized H_2 costs to the assumed cost of capital (and consequently, the capital charge factor (CCF)) at 10 locations identified in Figure 5, for the 2030 cost scenario described in Table 1 and Table S 4. The capital charge factor, which is used to calculate annualized capital costs of various technologies, is derived from the cost of capital using a 20 year technology/project lifetime. The value of CCF for the cost of capital of 5%, 8.1% and 12% corresponds to 8.0%, 10.3% and 13.3%, respectively.

Supplemental References

1. Shaner, M.R., Atwater, H.A., Lewis, N.S., and McFarland, E.W. (2016). A comparative technoeconomic analysis of renewable hydrogen production using solar energy. Energy Environ. Sci. *9*, 2354–2371.

2. Eichman, J., Townsend, A., and Melaina, M. (2016). Economic Assessment of Hydrogen Technologies Participating in California Electricity Markets (National Renewable Energy Laboratory (NREL)).

3. National Renewable Energy Laboratory (NREL) (2018). H2A: Hydrogen Analysis Production Case Studies. https://www.nrel.gov/hydrogen/h2a-production-case-studies.html.

4. Denholm, P., and Hand, M. (2011). Grid flexibility and storage required to achieve very high penetration of variable renewable electricity. Energy Policy *39*, 1817–1830.

5. Kopp, M., Coleman, D., Stiller, C., Scheffer, K., Aichinger, J., and Scheppat, B. (2017). Energiepark Mainz: Technical and economic analysis of the worldwide largest Power-to-Gas plant with PEM electrolysis. Int. J. Hydrogen Energy *42*, 13311–13320.

6. National Renewable Energy Laboratory (NREL) (2019). National Solar Radiation Database (NSRDB). https://nsrdb.nrel.gov/.

7. Sandia National Laboratories (2018). PV Performance Modeling Collaborative.

8. Leeuwen, C. van, and Zauner, A. (2018). Report on the costs involved with PtG technologies and their potentials across the EU.

9. Mayyas, A., Ruth, M., Pivovar, B., Bender, G., and Wipke, K. (2019). Manufacturing Cost Analysis for Proton Exchange Membrane Water Electrolyzers (National Renewable Energy Laboratory).

10. International Renewable Energy Agency (2019). Hydrogen: A Renewable Energy Perspective.

11. Saba, S.M., Müller, M., Robinius, M., and Stolten, D. (2018). The investment costs of electrolysis – A comparison of cost studies from the past 30 years. Int. J. Hydrogen Energy *43*, 1209–1223.

12. Thema, M., Bauer, F., and Sterner, M. (2019). Power-to-Gas: Electrolysis and methanation status review. Renew. Sustain. Energy Rev. *112*, 775–787.

13. ITM Power (2019). Interim Results Presentation.

14. Fu, R., Feldman, D., Margolis, R., Woodhouse, M., and Ardani, K. (2017). U.S. Solar Photovoltaic System Cost Benchmark: Q1 2017.

15. National Renewable Energy Laboratory (NREL) (2018). Annual Technology Baseline. https://atb.nrel.gov/electricity/2018/.

16. Eichman, J., and Flores-Espino, F. (2016). California Power-to-Gas and Power-to-Hydrogen Near-Term Business Case Evaluation (National Renewable Energy Laboratory (NREL)).

17. Tietze, V., Luhr, S., and Stolten, D. (2016). Bulk Storage Vessels for Compressed and Liquid Hydrogen. In Hydrogen Science and Engineering : Materials, Processes, Systems and Technology (Wiley-VCH Verlag GmbH & Co. KGaA), pp. 659–690.

18. Ahluwalia, R.K., Papadias, D.D., Peng, J.-K., and Roh, H.S. (2019). System Level Analysis of

Hydrogen Storage Options (Argonne National Laboratory).

19. Amos, W. (1998). Costs of Storing and Transporting Hydrogen (National Renewable Energy Laboratory).

20. Lord, A.S., Kobos, P.H., and Borns, D.J. (2014). Geologic storage of hydrogen: Scaling up to meet city transportation demands. Int. J. Hydrogen Energy *39*, 15570–15582.

21. Forsberg, C. (2006). Assessment of Nuclear-Hydrogen Synergies with Renewable Energy Systems and Coal Liquefaction Processes (Oak Ridge National Laboratory).

22. Penev, M., Rustagi, N., Hunter, C., and Eichman, J. (2019). Energy Storage: Days of Service Sensitivity Analysis (National Renewable Energy Laboratory (NREL)).

23. U.S. Environmental Protection Agency (2018). Greenhouse Gas Reporting Program (GHGRP). https://www.epa.gov/ghgreporting/ghg-reporting-program-data-sets.

24. Hart, W.E., Laird, C.D., Watson, J.-P., Woodruff, D.L., Hackebeil, G.A., Nicholson, B.L., and Siirola, J.D. (2017). Pyomo — Optimization Modeling in Python (Springer International Publishing).

25. Gurobi Optimization, L. (2018). Gurobi Optimizer Reference Manual. http://www.gurobi.com.